LAND-USE LAND-COVER CHANGE AND THE EFFECTS ON HYDROLOGY OF THE NORTH RIVER BASIN, ALABAMA

by

KORY JAMES PILET

NICHOLAS R. MAGLIOCCA, COMMITTEE CHAIR
SARAH J. PRASKIEVICZ
JOHANNA ENGSTRÖM

A THESIS

Submitted in partial fulfillment of the requirements
for the degree of Master of Science
in the Department of Geography
in the Graduate School of
The University of Alabama

TUSCALOOSA, ALABAMA

2019

ABSTRACT

Land-use and land-cover (LULC) change is a continuous and dynamic process that is driven by human-induced activity. The North River watershed, located in Alabama, exemplifies patterns of forestry practices related to commercial logging that are present with the increasing frequency of intensive forestry practices across the Southeastern U.S. While many studies focus on expanding urbanization within watersheds and the effect on hydrology, there is a need to study effects on hydrology of newer forestry practices, which promote shorter regeneration and growth periods with more frequent tree harvest. Using the Soil and Water Assessment Tool (SWAT), a GIS hydrologic modelling program using watershed data (LULC, soil weather, elevation), a calibrated and validated model (NSE: 0.74 and 0.63, respectively) was produced and run for the study period of 2001-2018. LULC change trends between six NLCD LULC change periods (2001 to 2004, 2004 to 2006, 2006 to 2008, 2008 to 2011, 2011 to 2013, and 2013 to 2016) were examined and the impact on both discharge and water-balance components were analyzed. Using a KS-test on the distribution of climate de-trended monthly simulated discharges, three LULC change scenarios revealed statistically different distributions. With net forest loss in the watershed, water yield and subsequent discharge values increased; scenarios with forest gain resulted in water yield and discharge decreasing through various water-balance components analyzed in SWAT. These results suggest that LULC change can have effects on the hydrologic cycle with impacts on water yield through alteration of the water-balance variables.

DEDICATION

This thesis is dedicated, first, to my parents, Kerry and Jacqueline Pilet. Without their endless love, support, and guidance through the highs and lows of college, this would not be possible. To all of my friends and colleagues, their words of encouragement and wisdom throughout the process have made this as seamless as ever. To my advisors, they have helped me along every step of the way and I cannot thank them enough for that.

LIST OF ABBREVIATIONS AND SYMBOLS

LULC	Land-Use and Land-Cover
ENSO	El Niño Southern Oscillation
NAO	North Atlantic Oscillation
PNA	Pacific North American
AMO	Atlantic Multidecadal Oscillation
AO	Arctic Oscillation
GIS	Geographic Information Systems
SWAT	Soil and Water Assessment Tool
U.S.	United States
NLCD	National Land Cover Dataset
Km^2	Square kilometers
m^3/s	Cubic meters per second
MRLC	Multi-Resolution Land Characteristics
SWAT-CUP	Soil and Water Assessment Tool – Calibration and Uncertainty Program
ARS	Agricultural Research Service

USDA	United States Department of Agriculture
CREAMS	Chemicals, Runoff, Erosion for Agriculture Management Systems
GLEAMS	Groundwater Loading Effects on Agriculture Management Systems
EPIC	Environmental Impact Police Climate Model
SWRRB	Simulator for Water Resources in Rural Subbasins
ROTO	Routing Outputs to Outlet Model
HRU	Hydrologic Response Unit
SCS-CN	Soil Conservation Service – Curve Number
DEM	Digital Elevation Model
NRCS	National Resource Conservation Service
NSE	Nash-Sutcliffe Efficiency
SUFI-2	Sequential Uncertainty Fitting
95PPU	95% Prediction Uncertainty
SSURGO	Soil Survey Geographic Database
CDF	Cumulative Distribution Function
KS	Kolmogorov-Smirnov
ET	Evapotranspiration
SW	Soil Water

PERC	Percolations
GW_RCHG	Groundwater Recharge
SURQ	Surface Runoff
LATQ	Lateral Flow
GW_Q	Groundwater Flow
WYLD	Water Yield

ACKNOWLEDGEMENTS

I am humbled and grateful for the opportunity that has been presented to me. I would like to thank the Department of Geography, the faculty of the University of Alabama, and fellow colleagues within the field of science for the endless assistance, support, and encouragement that undoubtedly helped me the last couple of years. I am most beholden to my advisors: Dr. Nick Magliocca for the endless hours spent in his office discussing the next course of action, Dr. Sarah Praskievicz for the weekly phone calls and SWAT modeling advice, and Dr. Johanna Engström for her unmatched knowledge on the climate and hydrology of the Southeast. Without their crucial input, stimulating scientific questions, and willingness to guide me through the rigorous world of science, I am not sure this project would be what it is today.

CONTENTS

LIST OF TABLES

LIST OF FIGURES

INTRODUCTION

Land-use and land-cover (LULC) change has been an activity performed since the beginning of human-kind leading to changes in hydrologic regimes worldwide. The frequency and extent of anthropogenic LULC change has increased in the last several decades exacerbating the need to understand the effects of LULC change in highly modified watersheds. Land-cover is not static, but often undergoes constant and ongoing change, including: clearcutting vegetation for grazing/cropping or regrowth of plantation forests (Watson et al., 2014). Rapid LULC change is often driven by market desires, which can result in deleterious impacts on the environment and water resources of a watershed. Changes in land cover result in both immediate environmental impacts through rainfall-runoff characteristics but also result in longer-term changes in ground water regimes (Choto and Fetene, 2019). Evapotranspiration, interception, infiltration, and runoff are affected through morphological and physiological changes of land cover (Zhang et al., 2018). A growing number of populations across the globe are becoming more acquainted with water-quantity and water-quality problems triggered by changes in land cover and climate, the largest drivers of hydrological variations (Arceo et al., 2018; Zhang et al., 2018). With a continually growing population reliant on a resource that is vulnerable to the impacts of LULC change, producing deleterious effects on water resources, it is paramount for resource managers to understand how these many factors work in conjunction for water security purposes.

A watershed is an area of land where rainfall and snowmelt drain into a stream network that flows through a single outflow point. Watersheds provide water resources for domestic,

agricultural, and ecological maintenance, a necessary resource for organisms throughout the trophic levels. Runoff, infiltration, and evapotranspiration within watersheds are critical components of the water cycle, where precipitation returns to the ocean, a location where the majority of evaporation in the initial stage of the water cycle begins (Gleick, 1996). Forested watersheds in the Southeast U.S. provide drinking water through surface and groundwater sources for over two-thirds of the population. The United States in general is reliant on forested watersheds for the majority of public and private water sources, where more than 75% of them are first order streams (Suttles et al., 2018). Forested watersheds buffer the cyclical nature of rainfall, by storing water through infiltration into the soil and groundwater, while also providing water during droughts by sustaining baseflow to rivers (Price, 2011). In contrast, heavily modified land-cover in watersheds lead to a whole array of changes in both water quantity and quality by restricting stream/land/vegetation infiltration from rainfall excess. The current scientific consensus is that: reduction in forest cover produces an increase in water yield and amplified stormflow runoff variability while increases in forest cover reduce water yield and dampens stormflow runoff variability (Vertessy et al., 2001). The Southeastern U.S. has seen strong urban growth and associated economically driven land use changes that alter watersheds and their hydrologic regimes. Expansion of urban and suburban habitats result in fragmented non-urban habitats, which has occurred in more than 95% of the watersheds in the northern hemisphere (Singh et al., 2018). Urban extent of the nine Southeastern U.S. states is projected to double in the next 40 years (Suttles et al., 2018). Combining the reduction of forest-cover trends in the Southeastern U.S. with the growing population will only further stress water resources.

Climate regimes and land-cover types are the largest anthropogenically affected factors that influence hydrology of a river basin. As discussed earlier, LULC change is superimposed over a larger climatic trend that can be attributed partially to atmospheric teleconnections as well as anthropogenic climate change (Engström and Waylen, 2017; Portmann et al., 2009). Since the focus of this research is assessing the contribution of LULC change to hydrological changes, identifying the atmospheric teleconnections that influence climate across the Southeast and drive streamflow is necessary to understand the role it plays in addition to LULC change (as well as de-trending for climate over the study period will be of utmost importance). The main meteorological teleconnections that have some level of influence on the Southeastern U.S. as reported by Engström and Waylen (2018) are the El Nino-Southern Oscillation (ENSO), the North Atlantic Oscillation (NAO), the Pacific-North American pattern (PNA), and the Atlantic Multidecadal Oscillation (AMO), most of which are strongly seasonal and widely varying. The AMO is a low-frequency sea-surface oscillation between warm (positive) and cool (negative) phases, running on a 60 to 80-year periodicity. AMO influence on precipitation is greatest in the winter months with positive phases associated with decreased precipitation regimes across the Southeast U.S. (Schlesinger and Ramankutty, 1994; Enfield et al., 2001). The AO is an index measuring the strength of atmospheric circulations in the middle and upper latitudes, particularly at the poles. A positive AO phase is characterized by below-average air pressure over the Arctic with higher than average air pressure over the Pacific and Atlantic Oceans. A negative AO phase has higher than average air pressure over the Arctic region with lower than average air pressure over the Atlantic and Pacific Oceans (Thompson and Wallace, 1998; Dahlman, 2009). According to Engström and Waylen (2018), there is a significantly positive correlation between AO and precipitation in the Southeastern U.S., indicating a wetter regime during positive phases

and drier during negative phases with peak influence during fall and winter, but increased rainfall is negated by warmer temperatures and higher evapotranspiration, resulting in little overall change in streamflow. The NAO is a variation in strength of the Icelandic low pressure and Azores high pressure system, often having variability on the order of weeks (Hurrell, 2003; Yamazaki et al., 2019). Conflicting research shows that the NAO has significant influence on precipitation and temperature in the Southeast during fall and winter seasons (Katz et al., 2003) while other research has shown that there is a weaker influence with little seasonality (Engström and Waylen, 2018). The final two teleconnections are tied more closely together with each influencing the other: ENSO and PNA, where the latter is driven by the former (Li and Xiao, 2018). According to Rasmusson and Wallace (1983), ENSO is a phenomenon characterized by anomalous sea surface temperatures in the equatorial Pacific (warmer sea surface temperatures being El Niño and cooler than normal being La Niña), and these events help drive a positive PNA (El Niño) or a negative PNA (La Niña) per Li and Xiao (2018). The PNA is characterized by positions of troughs and ridges over the continental United States; a positive PNA is defined by a trough in the Northwest Pacific Ocean with a downstream ridge over the Rocky Mountains and trough over the Eastern U.S. (Blackmon et al., 1984; Leathers et al., 1991). The reversal of this pattern is then defined as a negative PNA with ridging over the Northwest Pacific Ocean, a trough in the Rocky Mountains, and a ridge over the Eastern U.S. (Blackmon et al., 1984; Leathers et al., 1991). El Niño is often correlated strongly with increased precipitation in the late fall and winter months in the Southeastern U.S., although it is noted that on less frequent occasions, El Niño reflects a drier signal when looking at precipitation which can be attributed to fewer tropical systems (Engström and Waylen, 2018). The teleconnection signals can be identified in the streamflow, meaning surface and subsurface hydrology are strongly influenced,

especially by AMO and ENSO, making it important to account for when monitoring streamflow and producing hydrological forecasts.

The complexity of watersheds, including the intertwined nature of land-cover change and climate, and the hydrologic cycle are simplified through geographic information systems (GIS) based hydrologic modelling. The nonlinear behaviors of many hydrological parameters (climate, land-cover change, etc.) make each watershed and the associated parameters unique (Zhang et al., 2018). In the case of the North River watershed, the Soil and Water Assessment Tool (SWAT) is selected as the model of choice due to its popularity and reliability in predicting hydrologic scenarios. SWAT has emerged as a premiere semi-distributed hydrologic model, with well-documented success in modelling watershed hydrology and water quality as well as ecosystem services with over 3,000 published articles (Tan et al., 2019). The algorithms programmed into SWAT are simple but are derived from physical principles of hydrology. As noted by Yaduvanshi et al. (2018), a few major strengths of SWAT are due to its semi-distributed nature: (1) the computational efficiency due to these simplified algorithms, (2) GIS interface, (3) incorporation of data, and (4) the ability for it to capture much smaller hydrologic changes. One drawback to SWAT is the need for highly detailed spatial data for model set up and calibration (Yaduvanshi et al., 2018). This drawback is not one that hinders the choice of using SWAT modelling as the North River basin has adequate elevation, meteorological, and soil data. Using SWAT-CUP, a calibration and validation program for SWAT models, the sensitivity of parameters is assessed, and those deemed sensitive are adjusted toward the optimal values in the North River watershed. But the concern of uncertainty must be rigorously accounted for, due to the multitude of algorithms and parameters that contribute to the modelling simplification process.

Studies of Southeastern U.S. watersheds show that the signal of forest clearing or thinning is seen in the discharge of a river and is most notable during the first-year water yield (Sun et al., 2015). Grace et al. (2006) found that thinning of a pine plantation doubled water yield with a strong signal in drier years. Discharge in a watershed dominated by pine stands showed a correlation with increased discharge during the growing season when thinned or cleared; models developed that show that lower basal area (driven by forest thinning or clearcutting) of forest stands in the Southeast can lead to >50% more water yield (Sun et al., 2015). Stand plantations, grown for the primary purpose of bioenergy feedstock and saw timber, exhibit a patch-work mosaic of uneven aged hardwood, mixed hardwood-pine, and evergreen stands (Asaro et al., 2017). These patchwork stands in the Southeastern U.S. have seen the density of tree planting decrease by nearly 50% from the 1950s to early 2000s in commercial forest plantations, as a part of intensive forestry practices to promote quicker growth in concert with herbicides and pesticides (Asaro et al., 2017). A cyclical trend of increased spatial coverage of shrub/grassland and decreased forest coverage noted by NLCD analysis in ArcMAP, a GIS software program, is associated with forest stand removal for commercial timber use. The reciprocal of that pattern of patch-work shrub/grassland replaced by forest is regrowth of stands through intensive forest management as described earlier. Through SWAT, these repetitive LULC changes were simulated with realistic meteorological forcings in order to simulate discharge in a dynamically changing basin, for analysis of LULC change effects on both seasonal and monthly level discharge.

The North River watershed is a mixed-use, small to medium sized rural watershed with cyclical clearcutting, logging, and agriculture as the dominating land-cover types, within the state of Alabama. This watershed has not seen the large urban growth that many of the more

urban and suburban watersheds across the Southeast U.S. have seen (Suttles et al., 2018). The oscillating spatial extent of evergreen, deciduous, and mixed forest land-cover types match the pattern of intense forestry of both pine-hardwood stands and loblolly pine stands, the dominant evergreen timber species in the Southeastern U.S. (Griffiths et al., 2017; Laiho et al., 2003). Silvicultural practices in the region have trended toward short rotation stands (10-15 years) with whole tree harvest of pine plantations. Land cover types under this scenario are often subjected to more intensive management including mechanical and chemical preparation of clear-cut stands and more frequent harvest (Griffiths et al., 2017). Stand harvest and site preparation in these intensive silvicultural practice areas contribute to the changes in hydrology, both water quantity and quality, by altering evaporation/evapotranspiration mechanisms as well as infiltration mechanisms driven primarily by vegetative land-cover removal (Griffiths et al., 2017). It is imperative to study the effects of LULC change on a watershed that not only provides a water source for the public, but is unique in LULC (not heavily urbanized but extensive timber harvesting) and geology (underlain by two wholly different geologic formations). Most of the prior studies have focused on urbanizing watersheds and water quality/quantity from urbanization, but rural watersheds with changing timber harvest practices must be assessed for major hydrologic changes. The high temporal resolution of LULC change, through the use of NLCD products, provides useful data to pinpoint changes in these fast growing, intensive forestry stands. This research focuses how land cover has changed in the North River watershed and more specifically, how that change has affected the water quantity or discharge of the North River. Parsing out the climate signal is important since it can profoundly impact hydrology and water resources, as it was noted by Zipper et al. (2018) that impacts of LULC change are superimposed on a larger climate trend which can either amplify or counter

the impacts of climate change; each watershed needs to be taken on an individual basis. This research will be accomplished through the application of the Soil and Water Assessment Tool (SWAT) and statistical methods commonly applied to hydrological output. The use of GIS, SWAT, spatial, and temporal data is done in order to tackle the two main questions of this study: what are the changes in land cover through the study period (2001-2018) and what are the subsequent changes in discharge and water-balance components during that time period? The result of this project is to provide solid scientific findings that watershed agencies may use to formulate management practices that may directly and indirectly affect future water security of the North River watershed.

RESEARCH METHODOLOGY

Study Area

The North River watershed extends from the headwaters in Fayette County, Alabama, to the Lake Tuscaloosa dam at the Black Warrior River junction (O'Neil et al., 2010). For the purpose of this study, the core of the watershed analyzed was from the U.S.G.S. gage in Samantha, Alabama, near the entrance into Lake Tuscaloosa, north into Fayette County, an area roughly 577 km^2 (Fig. 1). The watershed is nearly 38 kilometers long and 23 kilometers at its peak width. The northern and eastern parts of the watershed are underlain by the Pottsville formation and drain the physiographic region known as the Cumberland Plateau. The western and southern portions of the watershed are in the Fall Line Hills area underlain by the Coker formation of the Gulf Coastal Plain (O'Neil et al., 2010). The Pottsville formation is primarily sandstone, shale, and mineable coal deposits with streams occurring in steep-sided valleys due to the faulting and folding during the Pennsylvanian era. The Fall Line Hills region is a crescent-shaped band extended from Northwest Alabama through West/Central Alabama and into Eastern Alabama, where topography is less rugged than the Cumberland Plateau. The elevation map of the North River watershed provided in Fig. 2 outlines the higher elevation northern and eastern parts of the watershed's headwaters with lower elevation in the western and southern regions. The watershed is in a region where the Pottsville formation dips below the surface, overlain by the Coker Formation, a predominately sandy unit of both detrital deposits (sand and silt) and

marine deposits (carbonate/limestone) commonly found in the Gulf Coastal Plain (O'Neil et al., 2010). The Coker Formation of the Gulf Coastal Plain is loosely compacted and undeformed, indicating little active geologic faulting during the deposition of the formation, leading more permeable, continuous stratigraphy. This unique geology of the North River watershed is what drives stream routing processes.

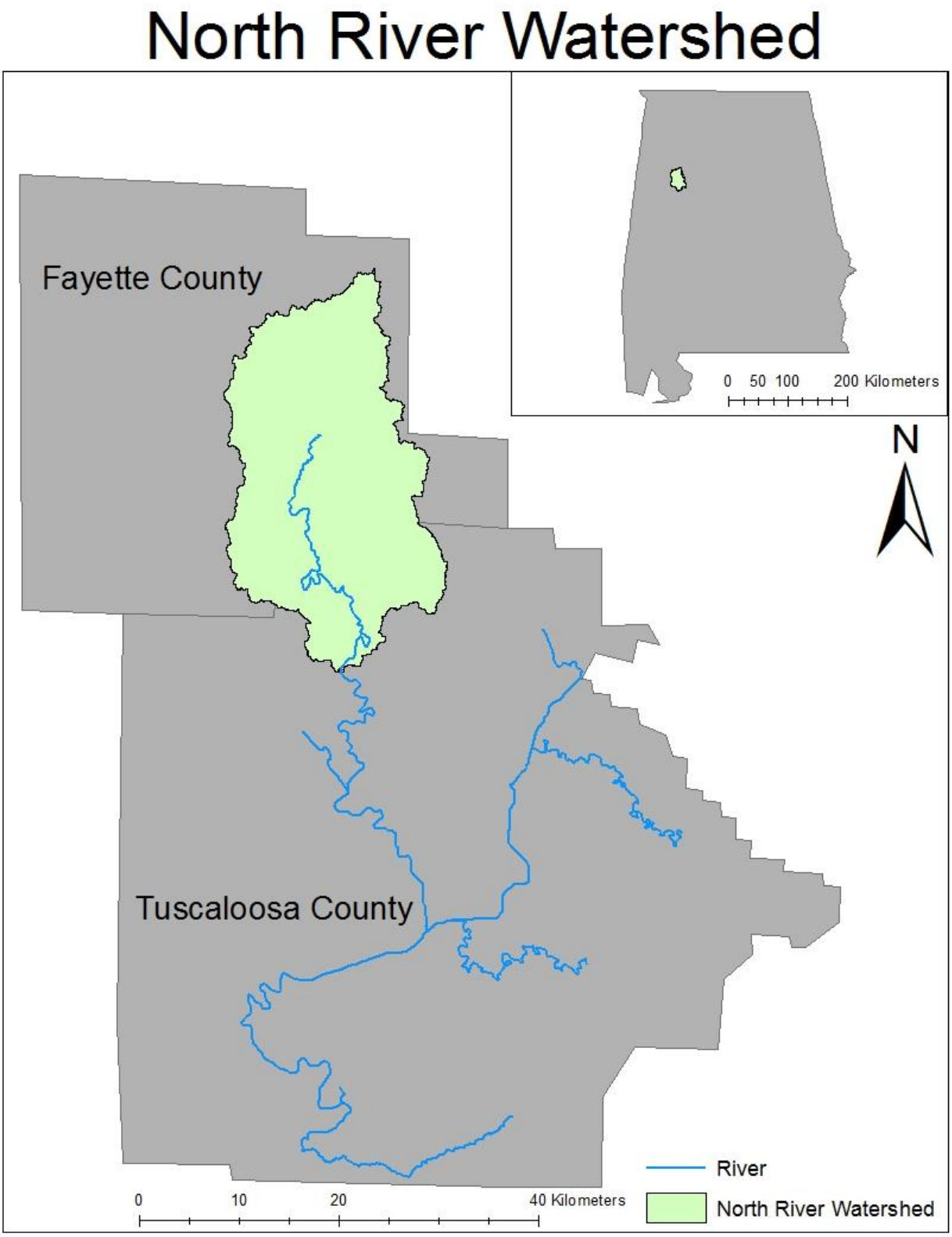

Figure 1: North River Watershed Boundary Map. The North River watershed is outlined in Tuscaloosa and Fayette Counties. Location of the watershed in the state of Alabama is shown in the upper right-hand corner of the map.

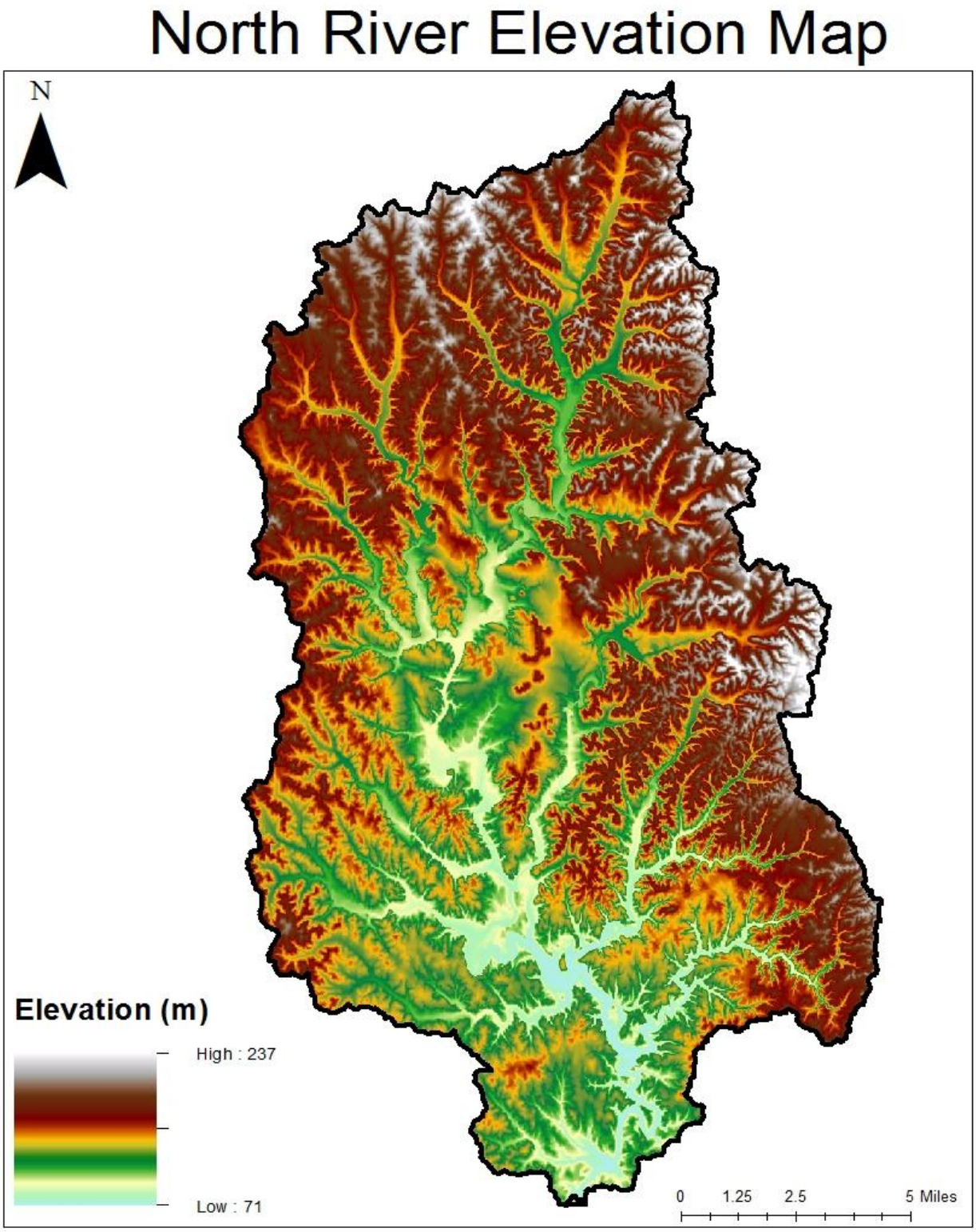

Figure 2: North River Watershed Elevation Map. Higher elevations associated with the Cumberland Plateau physiographic regions (north and east) while lower elevations are associated with the Fall Line Hills physiographic regions (west and south).

The drainage pattern of the North River is similar to many of the streams in the Southeastern U.S., possessing a dendritic geometry. Streamflow is sustained yearlong in a few larger tributaries and main channel, but many of the headwater tributaries in the northern extent of the watershed are ephemeral and receive no baseflow during the summer and fall months due to the relatively impermeable Pottsville shale formation (O'Neil et al., 2010). Tributaries flowing from the western Fall Line Hills region flow yearlong due to the sand and gravel aquifers. Average daily flows show that September on average has the lowest flow with February having the highest flow per O'Neil et al. (2010). Slack (1987) quantified that the majority of the discharge feeding into Lake Tuscaloosa is from the North River (59%) with the rest coming from nearly a dozen smaller creeks and ungauged tributaries. With the creation of Lake Tuscaloosa, one of the largest reservoirs in Alabama, in 1971, the North River has become a vital watershed supplying most of the discharge for a significant public water source for the city of Tuscaloosa.

The North River watershed is a mixed-used watershed, with the largest land-cover classes being pasture, shrub, and forests. Per O'Neill et al. (2010), resource extraction is a major source of income within the North River watershed; this includes, but is not limited to logging, agriculture, mining, and livestock. There are several major highways that run through the watershed as well as the urban center of Berry, Alabama, a town of roughly 1,200 people per the 2010 U.S. Census. These many land-cover types strongly influence the water quality and quantity that flows into Lake Tuscaloosa, a reservoir serving as the public water source for the Tuscaloosa, Alabama, region. The North River watershed is subject to LULC change commonly associated with industry/agriculture as well as meteorological teleconnections that influence the precipitation and temperature patterns. Despite the majority of the watershed being covered by

either forest or shrub/grassland vegetation as classified by the National Land Cover Database, a mapping product of land-cover and land use derived from Landsat imagery, economic factors drive the land-cover. As noted by O'Neil et al. (2010) at the Geological Survey of Alabama, a plurality of the natural forest coverage has been converted to evergreen stands with shrub/grassland/developed open-space patches as a successional stage to clearcutting and logging, reflecting the strong influence resource extraction has on the local economy and LULC change.

The climate of Alabama, and the Southeastern U.S., is classified as a humid subtropical climate using the Köppen classification system (Norrell and Gomillion, 2019). There are four distinct seasons with most precipitation coming from mid-latitude weather systems and summer convective processes. Using the nearest official National Weather Service gauging station, Tuscaloosa, Alabama, Airport (KTCL), on a 30-year running average (1981-2010), the annual temperature is about 18 °C, with the summer average reaching 24 °C and the winter average dipping to 11 °C. The average annual precipitation is near 1,335 mm. The driest month is August with the wettest month being January (Fig. 3). Despite Alabama being characterized as a humid subtropical climate, recurring droughts have occurred twice in the last decade alone (2007 and 2016). With climate being the primary driver of streamflow (Campbell et al., 2011), it is important to note the climate regime of the North River watershed.

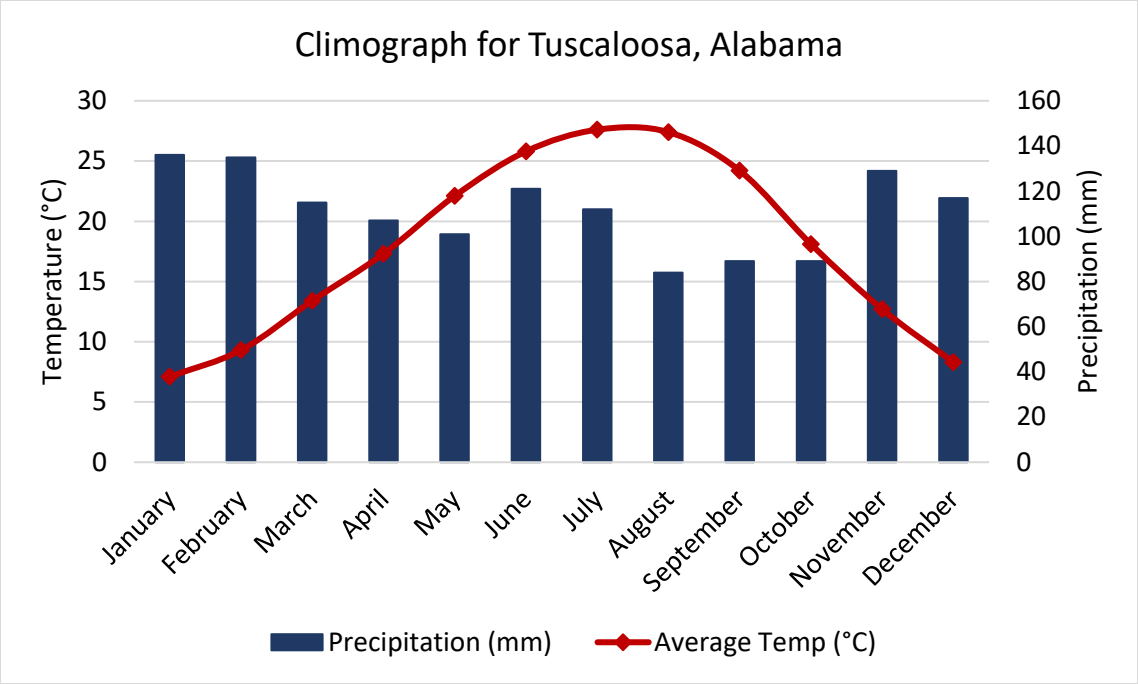

Figure 3: Climograph for Tuscaloosa, Alabama. Provided by the National Weather Service (from gauging station at the Tuscaloosa County Airport). Strong seasonality of temperature is shown with no general seasonal variability of rainfall.

Methods

The ArcGIS program (10.1) and Arc SWAT 2012 (Soil and Water Assessment Tool) were used to model discharge from the North River basin. Data input into the model included: land-use, soil, topography, and weather data. The data were then used to calibrate and validate the model using SWAT-CUP, a calibration, validation, and uncertainty parameter software program. Various land use scenarios from 1992 through 2016 were used to assess the impact of land use on discharge of the North River.

SWAT is a hydrologic model that operates on a daily timestep with the objective of predicting discharge, sediment, and various chemical yields of watersheds. Early development of SWAT can be traced back to the 1980s and three USDA Agricultural Research Service (ARS) modelling projects: (1) Chemicals, Runoff, and Erosion for Agricultural Management Systems

(CREAMS) which modeled the daily rainfall/hydrology component, (2) the Groundwater Loading Effects on Agricultural Management Systems (GLEAMS) which modeled the pesticide component, (3) and the Environmental Impact Policy Climate model (EPIC), which modeled the crop-growth component. Based on combinations of these three USDA-ARS models known as Simulator for Water Resources in Rural Subbasins (SWRRB), in addition to the USDA-SCS rainfall runoff modeling technology and Routing Outputs to Outlet (ROTO) model, SWAT was developed to reduce computing power and storage needs (Gassman et al., 2007). The physically based nature of SWAT, requiring specific information about input variables (soil, weather, topography), allows the model to directly simulate hydrologic properties using the input data. The ability to model dynamic temporal and spatial changes of best management practices, climate, LULC change, and other inputs and the impact on the watershed over a long time span (decades) was the primary goal of SWAT development (Neitsch et al., 2011). Improvements to the SWAT model since its development in the early 1990s include multiple hydrologic response units, snow melt and fertilizer/pesticide cycling improvements, bacteria transport, weather forecast scenarios, and most recently, improvements to the curve-number calculation through soil water contact and plant evapotranspiration (Neitsch et al, 2011). The accurate prediction of the hydrologic variables is done through the water-balance equation, the sole driving force of processes within the watershed.

Modeled variables within SWAT include hydrology, weather, sediment transport, soil temperature, crop growth, nutrients, pesticides, and agricultural management, but for the purposes of this study, the focus will be on the hydrologic component of the model (Arnold et al., 1998). The watershed that is delineated in the model can be divided further into sub-basins and hydrologic response units (HRUs) based on homogenous land-cover type, soil type, and

slope class (Quyen et al., 2014). The single most important algorithm within the model is the water balance equation:

$$SW_t = SW_0 + \sum_{i=1}^{n} (R_{day} - Q_{surf} - E_a - w_{seep} - Q_{gw})$$

Quyen et al. (2014) explained the variables within the water balance equation: SW_t is the final soil water content (mm), SW_0 is the initial soil water content on day *i* (mm), R_{day} is the amount of precipitation on day *i* (mm), Q_{surf} is the amount of surface runoff on day *i* (mm), E_a is the amount of evapotranspiration on day *i* (mm), W_{seep} is the amount of water entering the vadose zone from the soil profile on day *i* (mm), and Q_{gw} is the amount of return flow on day *i* (mm). This equation is used to model the flow of water into and out of the system, in this case, the North River watershed.

A key component of calculating the water balance equation in SWAT is the Soil Conservation Service Curve Number (SCS-CN) method. The CN method is a widely used empirical parameter for estimating surface runoff that is a function of watershed land cover, soil properties, and hydrologic conditions (Kim et al., 2010). It was developed by the USDA Natural Resources Conservation Service by monitoring runoff from small catchments with varying land cover types (Garen and Moore, 2005). Runoff plays a critical role in the water-balance equation and the hydrologic cycle by controlling how much water flows into streams and thus is important to model simulations and is generated by saturation excess and infiltration excess (Sitterson et al., 2017). In SWAT, the CN method is calculated using daily rainfall and retention, based on antecedent soil moisture and evaporation/evapotranspiration (Tasdighi et al., 2018). Long-term SWAT simulations using the CN method, performed for the purpose of water-availability analysis, have been tested in numerous scientific studies with overwhelming satisfactory results.

Data Acquisition and Processing

A digital elevation model (DEM), soil map, land-use/land-cover map, meteorological, and hydrological data were collected from various sources and input into SWAT. The Geospatial Data Gateway[1] was the source for the DEM, soil data, and land-cover data used for watershed building and model calibration. The DEM was developed by the U.S. Geological Survey, in 30-meter resolution format, which serves as a basis to delineate the watershed and calculate flow direction and accumulation in order to build stream networks. A slope map was produced from the DEM through ArcSWAT and five categories were produced: 0-10%, 10-20%, 20-30%, 30-40%, and >40% slope. These intervals were chosen to capture the lower-slope parts of the western watershed as well as the higher-slope northern and eastern parts of the watershed associated with the two different physiographic regions. The soil data, SSURGO, were downloaded in a database for the state of Alabama (NRCS, 2018). SSURGO is widely used due to the level of detail of soil geographic data from the National Cooperative Soil Survey (NRCS). Meteorological data from the official Tuscaloosa, Alabama, weather station (KTCL) were downloaded from the Global Weather Dataset[2] provided through Texas A&M as text files. This dataset was already formatted in SWAT text format which simplified inputting the data into the model. Daily temperature, solar radiation, relative humidity, wind, and precipitation data were acquired from 1979 through 2018. Data from the single USGS stream gage[3] in Samantha, Alabama, were used to calibrate and validate the model, and the gage was used as the watershed outlet in the delineation process. These stream-gage data were at the monthly time scale in ft^3/sec, but were converted to m^3/sec for calibration and validation process in SWAT-CUP. The

[1] https://datagateway.nrcs.usda.gov/
[2] https://globalweather.tamu.edu/
[3] https://waterdata.usgs.gov/al/nwis/uv/?site_no=02464000&PARAmeter_cd=00065,00060

last dataset needed for calibration was the 2011 National Land Cover Database (NLCD) produced by the Multi-Resolution Land Characteristics Consortium[4]. The NLCD is a 16-class land-cover classification that uses a decision-tree scheme to arrive at the land-cover classification categories from training data (Homer et al., 2007). Once all of these components were acquired, examined for missing data, and loaded into the ArcSWAT model, the model was then used to develop hydrologic response units (HRUs) and calculate sub-basin parameters.

HRUs are automatically defined by the model by lumping similar land-use, soil type, and slope characteristics within the defined thresholds for each category. There are more than 200 HRUs within each of the land-cover type scenarios in the North River SWAT model. The number of HRUs can be determined by the user, but are often only reduced in number for computational efficiency; for the purpose of this project, the number of SWAT-generated HRUs was not changed. Most simulations using the water-balance equation are performed at the HRU level due to the simplicity of lumping similar areas of the watershed into a single response unit. Because of this artifact of SWAT, HRUs are not a single continuous field and the water balance is calculated separately for each and then summed together to determine the hydrologic parameters for the sub-basin (Arnold et al., 2012). Sub-basins are user-generated (outlet is selected by user) and are defined from the DEM (sub-basin reach is defined from the elevation data in the same process in which watersheds are delineated). They are spatially distributed and streamflow flows from one sub-basin to another through routing properties established within the model (Kalcic et al., 2015). There are two sub-basins defined for this watershed: the upper sub-basin (~25% of the watershed) and lower sub-basin (~75% of the watershed). The watershed

[4] https://catalog.data.gov/dataset/usgs-national-land-cover-dataset-nlcd-downloadable-data-collection

was delineated into the sub-basins with the background knowledge of the northern headwaters having different stream characteristics (more ephemeral during summer and fall) as well as falling within the Cumberland Plateau physiographic region defined by the Pottsville geologic formation.

Calibration and Validation

For each simulation, a three-year initialization period was built into the model. This initialization period allows for parameters to reach acceptable indicator values before generating simulation data. These parameters in SWAT are generally soil moisture, aquifers, and reservoirs, which need to reach stable values before running; otherwise, the risk of underestimation of values may increase. The three criteria used to evaluate model fitness established by Moriasi et al. (2007) are Nash-Sutcliffe efficiency (NSE), R-factor, and P-factor. Parameters during calibration are adjusted to give the highest NSE (maximum of 1). The Nash-Sutcliffe will be the primary criterion that will be used to test for model fitness in this study and is referred to as the efficiency index (E_f) (McCuen et al., 2006):

$$E_f = 1 - \frac{\sum^n \left(\hat{Y}_i - Y_i\right)^2}{\sum \left(Y_i - \bar{Y}\right)^2}$$

in which $\hat{Y}_i$ = predicted values, Y_i = measured values, $\bar{Y}$= average of the measured values and n = the sample size of discharge values. The Nash-Sutcliffe numbers can range from -∞ to 1.0, where 1.0 indicates a perfect match of modeled discharge to observed discharge, computed as the ratio of residual variance to measured data variances, with a value >0.5 accepted as a sufficiently calibrated model (Nash and Sutcliffe, 1970). Once model parameters are optimized using the

NSE criteria, they are checked for overfitting which occurs when overparameterization in the calibration period results in a deterioration of model accuracy outside of the calibration period. Overfitting is checked for during model validation by using a separate dataset independent of the calibration period (Whittaker et al., 2010). After checking for overfitting, new optimized values for the parameters were updated in ArcSWAT using the manual calibration helper.

SWAT-CUP is a software program that combines four different algorithms for the optimization of parameters in a SWAT model: SUFI-2, GLUE, MCMC, and ParaSol. The SUFI-2 (Sequential Uncertainty Fitting Version 2) algorithm was used in this project to analyze sensitivity and uncertainty and to calibrate and validate many parameters (Thavana et al., 2018). If these parameters are not accounted for, large uncertainty and inaccuracies may arise with a hydrologic model. With the SUFI-2 algorithm, input parameter uncertainty is assumed to have a Gaussian distribution with the output uncertainty computed at the 95PPU or 95% prediction uncertainty level (Szezesniak and Piniewski, 2015). In this project, five iterations were run composed of 1500 simulations each with different parameter values sampled in the parameter space before optimization was reached. SWAT-CUP uses a Latin hypercube sampling of the parameter space during execution with post-processing computing the NSE for the watershed (Szezesniak and Piniewski, 2015). After each iteration, the new parameter ranges are narrowed to the suggested ranges and the next iteration commences with the goal of improving the fitness of the SWAT model. Parameters can be adjusted in three ways: replacement, relatively (as a percentage), and absolutely (add or subtract from current value). Parameters that vary absolutely are the groundwater parameters, where as those that vary spatially by HRUs are adjusted as a percentage, and replacement values are for those that do not vary with elevation, time, or space. The effective graphical representation of parameter sensitivity, best-fit values, and model results,

combined with the effective minimization of differencing between observed and simulated flows shows SWAT-CUP is an important contributor to hydrologic modelling.

Model calibration was done for the 2004-2014 period, with a three-year initialization period from 2001 to 2003. Using the land-cover from 2011, SSURGO soils, and the previously mentioned slope categorizations with the 30-meter DEM, the monthly simulated discharge was compared to the observed discharge at the Samantha, Alabama, U.S.G.S. gage station in SWAT-CUP. Model validation was also performed in SWAT-CUP for a period from 1992 to 1999, with a 2-year warm-up period from 1990 to 1991. The NSE values for the calibration and validation period are 0.74 and 0.63, respectively. These values show that the model performs well above the threshold that shows the model is sufficiently calibrated and is not overfitted (Fig. 4). The SWAT model for the North River basin can be used to accurately predict streamflow from the delineated North River watershed. Through sensitivity analysis of the North River SWAT model in SWAT-CUP, six parameters were identified as sensitive (p-value <0.05). These parameters with their ranges and fitted values are shown in Table 1.

Table 1
Parameters used for calibration, with absolute ranges and optimal (fitted) values.

Parameters	Description	Minimum	Maximum	Fitted
CN2 (Sub 1)	SCS runoff curve number	-0.1	0.1	-0.079583
CN2 (Sub 2)		-0.1	0.1	-0.149516
GWQMN	Depth of water in shallow aquifer	-1000	1000	-292.359
GW_DELAY	Groundwater delay in days	-30	90	3.559388
GW_REVAP	Groundwater movement from aquifer to unsatured zone	0.02	0.2	0.066184
SOL_K	Saturated hydraulic conductivity	-0.1	0.1	-0.056097
CANMX	Tree canopy storage	0	100	88.59769
NSE (Cal):	**0.74**			
NSE (Val):	**0.63**			

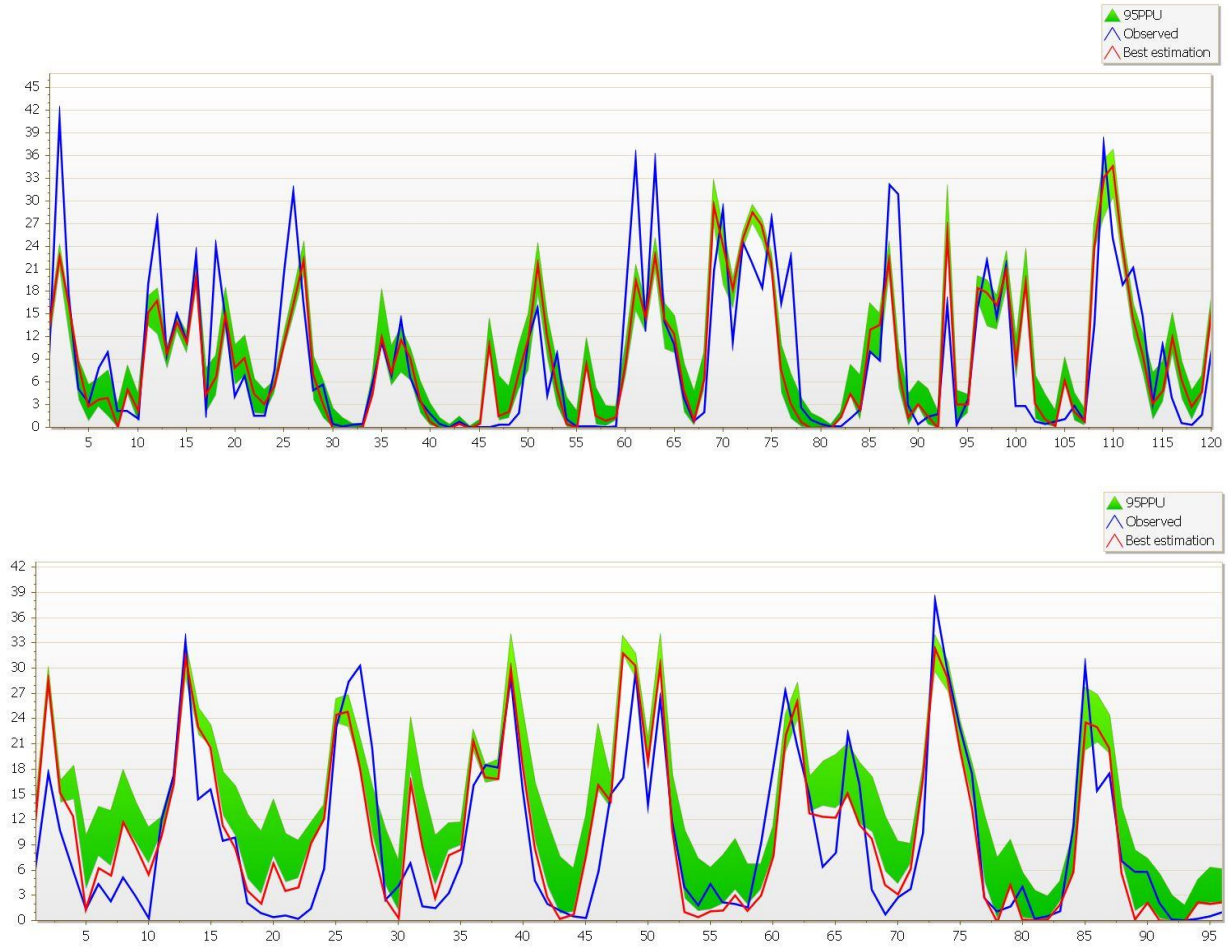

Figure 4: Calibration and Validation SWAT-CUP Plots. These two plots show the modeled (shown in red) and the observed (shown in blue) streamflow for the North River at the Samantha, Alabama, gage. Calibration is the top plot and validation is the bottom plot. These two plots show that the model on average predicts streamflow well in both the calibration (NSE: 0.74) and validation (NSE: 0.63) periods. The green shading represents the 95% probability distribution (95PPU) at the 2.5% and 97.5% levels of the CDF of simulated discharge (Abbaspour, 2015). Due to the inherent uncertainties with hydrologic modeling, the 95PPU encases 95% of any solutions that are simulated using the range of fitted parameters. The validation is an important complement to calibration, showing the model is not overfitted for the calibration period and that it is useful in all simulation scenarios.

Ground Truthing NLCD

The U.S. National Land Cover Database (NLCD) is produced by the Multi Resolution Land Characteristics Consortium (MRLC), a group of United States federal agencies that

generate land-cover products at a nationwide scale for the U.S. The 1992 NLCD was the first land-cover dataset produced for the continental U.S. by the MRLC at 30-meter resolution. The 1992 NLCD uses a 21-class legend adopted from the Anderson II classification system (Wickham et al., 2004). The MRLC implemented a 100-class unsupervised clustering algorithm to derive the 21-class classification system with manual editing to produce the final 1992 NLCD thematic map of land cover (Fry et al., 2008). The 2001, 2004, 2006, 2008, 2011, 2013, and 2016 thematic NLCD maps employ a decision-tree method for classification into 16 categories (Table 2). This change by the MRLC reflected improvements in technology and mapping methods; advantages included faster machine training, objectivity, set rules for classification confidence, and confidence mapping (Fry et al., 2008). The differences between the 1992 and post-2001 NLCD maps have resulted in large discrepancies in the datasets, but efforts have been made by Graham and Congalton (2009) to reclassify the 1992 NLCD into a legend compatible with the other NLCD products; the 1992 NLCD reclassification used the methodology established by Graham and Congalton (2009) for the purpose of climate de-trending in this study. Accuracy assessments done on the NLCD products from 1992, 2001, 2006, and 2011 show classification accuracies of those MRLC products have improved significantly since the 1992 release of the initial NLCD. The classification accuracies are as follows: 66% (1992), 79% (2001), 78% (2006), and 83% (2011) as shown by Wickham et al. (2004), Wickham et al. (2013), and Wickham et al. (2017). While the overall classification metrics of the NLCD thematic maps did not meet the benchmark established by Anderson et al. (1976), several individual classifications had satisfactory accuracy-assessment numbers (>85%): water, high intensity developed, deciduous and evergreen forests, shrubland, and cropland (Wickham et al., 2017). Because the North River is dominated by these land-cover types that had higher

classification accuracies, the NLCD is useful in tracking land-cover changes and the subsequent effects on hydrology within the North River basin.

Table 2: Aggregation of NLCD categories for LULC change analysis. The NLCD legend used is the 16-class classification and aggregation done based on CN.

NLCD Legend		Aggregated LULC Categories
11	Open Water	Water
21	Developed, Open Space	Urban
22	Developed, Low Intensity	Urban
23	Developed, Medium Intensity	Urban
24	Developed, High Intensity	Urban
31	Barren Land (Rock/Sand/Clay)	Barren Land (Rock/Sand/Clay)
41	Deciduous Forest	Forest
42	Evergreen Forest	Forest
43	Mixed Forest	Forest
52	Shrub/Scrub	Grassland/Range
71	Grassland/Herbaceous	Grassland/Range
81	Pasture/Hay	Agriculture
82	Cultivated Crops	Agriculture
90	Woody Wetlands	Wetlands
95	Emergent Herbaceous Wetlands	Wetlands

The NLCD classification scheme was used in this project with classifications for land-cover in the North River watershed including water, urban-open space, urban-low intensity, urban-medium intensity, urban-high intensity, barren land, deciduous/evergreen/mixed forests, shrubland, herbaceous grassland, pasture, crops, woody wetlands, and emergent herbaceous wetlands. For the purpose of the land-cover analysis, the urban, forest, shrubland/grassland, pasture/crops, and wetland categories were aggregated, as shown in Table 2, due to similar average curve number values provided by Hong and Adler (2008). Through zonal statistics in

ArcMap, analysis of areas of forest loss and forest gain with the goal of quantifying exact LULC change within the North River basin were performed.

LULC change analysis was performed using both ArcSWAT and a thematic change map through map-algebra techniques in ArcGIS. The majority of land-cover change in the watershed (>80%) is forest coverage (deciduous, evergreen, mixed) converted to range (scrub/shrub and grassland) or developed-open space. In conjunction with the previously mentioned LULC trend, reversal of that pattern from developed open space and range back to forest was also observed through NLCD analysis. Coordinates were produced, in a targeted methodology, for five different locations where forest changed to shrub/scrub or grassland land cover between the 2011 and 2016 NLCD and field verification was performed to note the present-day land cover (Fig. 5). The designated sites were visited and photographs taken. Figure 5 is a map with coordinate points of targeted ground truthing sites and Table 3 is a description of visited field locations with pictures. The sites visited focused on the forest to shrub/scrub or grassland change or former shrub/scrub or grassland that has now been converted to forest. Several other sites were assessed via Google Earth. Many of the transition sites, changing from forest to range, exemplified clearcutting and/or logging signatures, with uniform regrowth, also known as an even-aged stand, at younger stages than surrounding forest stands (Merrit, 1973; Silviculture Handbook). As noted by Xian et al., (2010), recovered forest clearcuts have been classified as shrubland/range within a 5-year regrowth period by NLCD classification methods. There were multiple and different-aged regenerated clearcut stands observed from field observations at selected points within the North River watershed that were identified as forest to shrubland/range transition, indicating the reliability of the NLCD to accurately identify major land-cover changes within the North River basin.

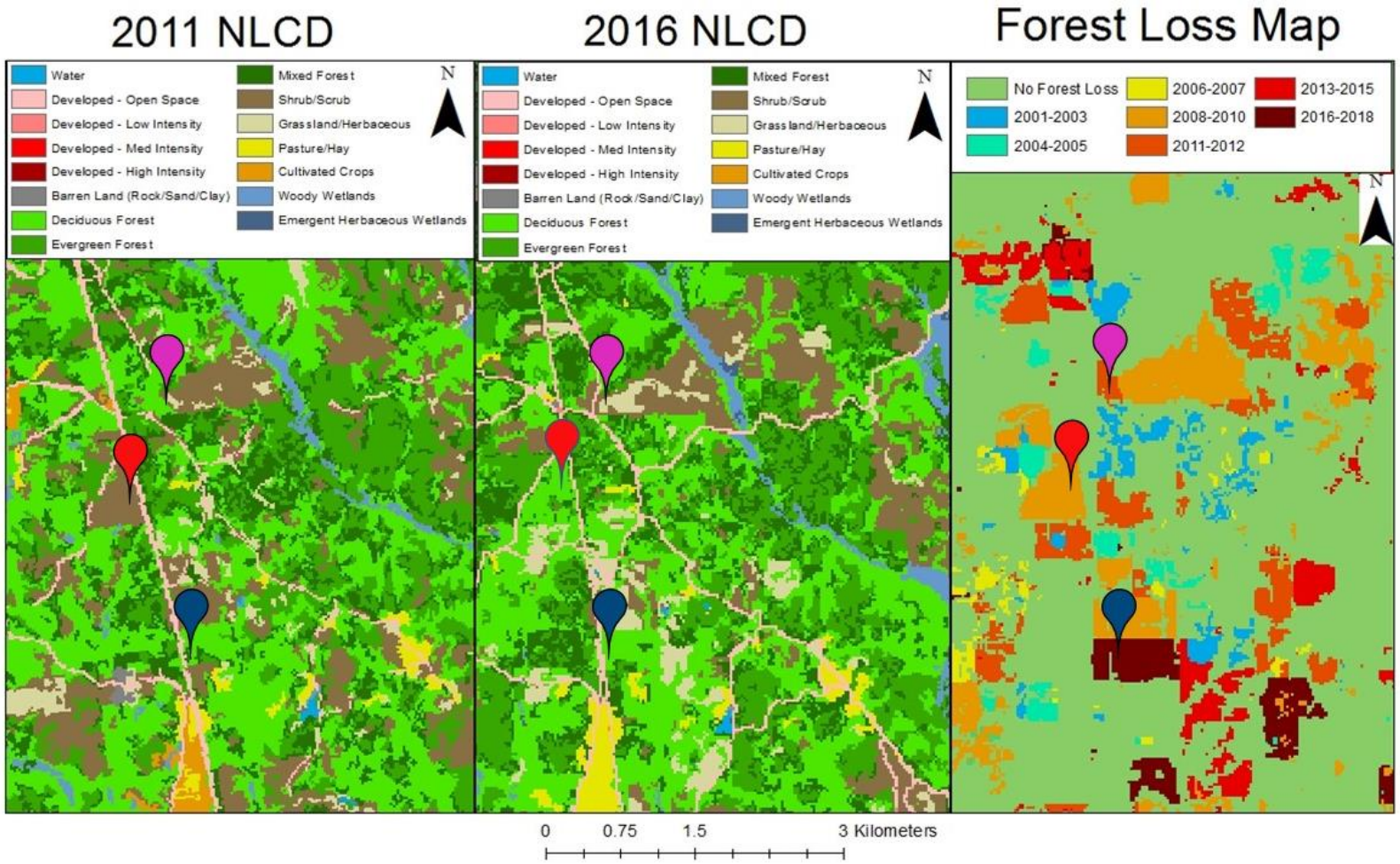

Figure 5: Field Verification Sites with Coordinates. The above locations show field-visited coordinates that have had clearcutting activity in the past. The visited points were based on changes that have been observed between the 2011 and 2016 NLCD as well as changes noted in the Hansen et al., (2013) Global Forest Change product[5] which shows the amount of forest lost broken down by NLCD increments.

[5] https://earthenginepartners.appspot.com/science-2013-global-forest

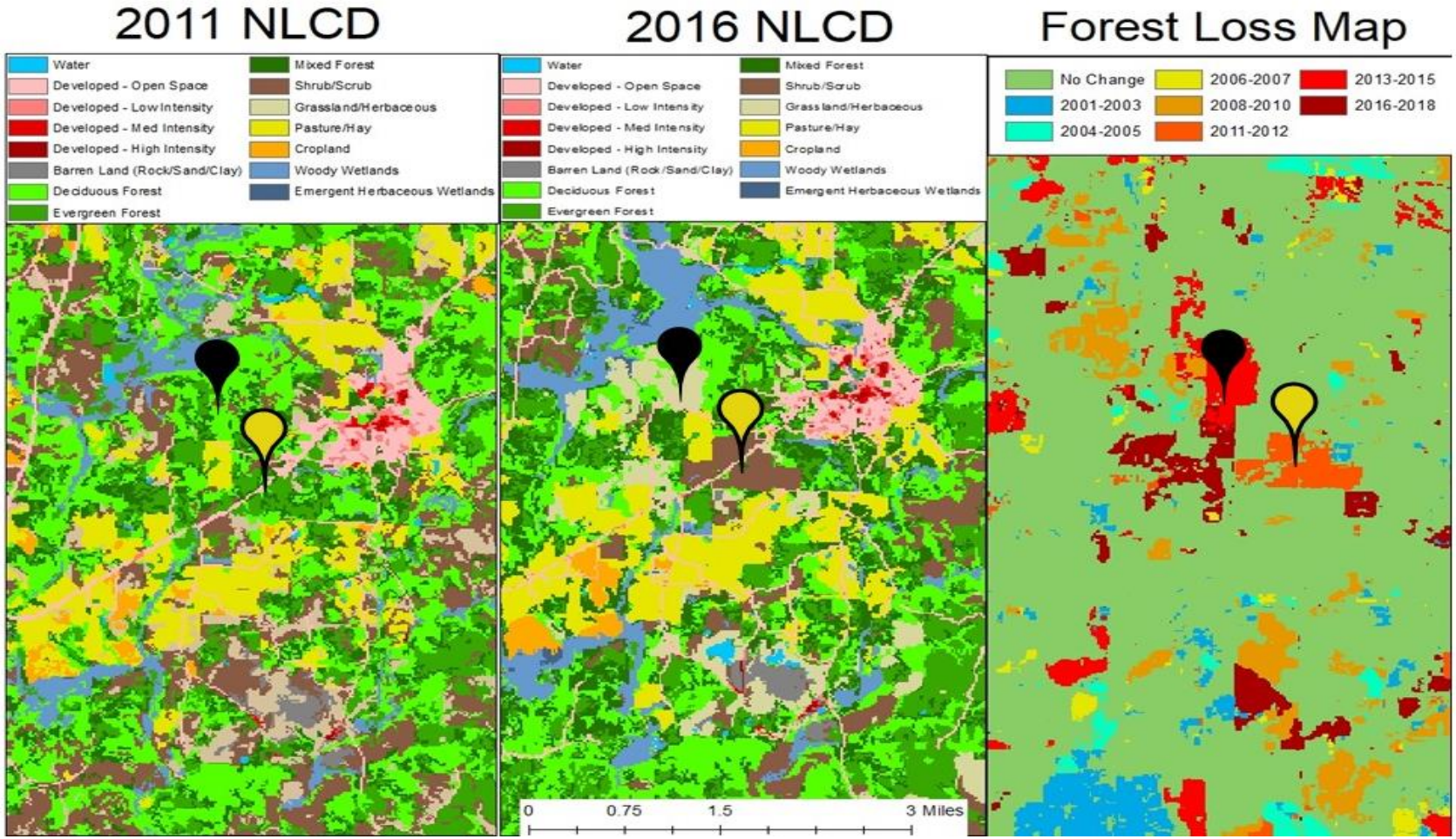

Figure 5: Field Verification Sites with Coordinates. The above locations show field-visited coordinates that have had clearcutting activity in the past. The visited points were based on changes that have been observed between the 2011 and 2016 NLCD as well as changes noted in the Hansen et al., (2013) Global Forest Change product[6] which shows the amount of forest lost broken down by NLCD increments.

[6] https://earthenginepartners.appspot.com/science-2013-global-forest

Table 3: NLCD field verification sites. Locations correspond to Figure 5.

Symbol	Latitude	Longitude	Picture
	33.755985	-87.649817	
Site Description: this site exemplified characteristics of a clearcut. Old growth trees in the background and foreground show much more variation in crown height with more uniform growth in the center part, where the former clearcut is located. Using the Global Forest Change product, this clearcut was done during the 2011-2012 timeframe with regrowth. This sight is classified as shrub/scrub in both the 2011 and 2016 NLCD with the addition of grassland classification where clearcutting was ongoing (although not visible from this perspective due to brush along the roadside).			
	33.731525	-87.648176	
Site Description: this site was a forested stand (as classified by the 2011 and 2016 NLCD) that was cleared after 2016, as indicated by the Global Forest Change product. This site shows the aftermath of a clearcut (1-2 years) and further reinforces the nature of cyclical clearcutting and forest stand recovery in the North River watershed. This image was taken by Google Earth street view in 2018.			

Table 3 Cont.: NLCD field verification sites. Locations correspond to Figure 5.

Symbol	Latitude	Longitude	Picture
	33.746358	-87.654599	 

Site Description: this site is an older clearcut with longer recovery since logging. Global Forest Change Product indicates stand clearing between 2008-2010. Approximate tree height was 20-25 feet. Relatively uniform crown height with underbrush regrowth common with older clearcuts not maintained through fire practices. Power line cut through recovering forest stand shows uniform growth. This site was classified as scrub/shrub in the 2011 NLCD with conversion to forest categorization in the 2016 NLCD. This, in addition to the polygonal nature of the clearings support the idea of forest stand logging.

<table>
<tr><td colspan="4">Table 3 Cont.: NLCD field verification sites. Locations correspond to Figure 5.</td></tr>
<tr><td>Symbol</td><td>Latitude</td><td>Longitude</td><td>Picture</td></tr>
<tr><td></td><td>33.657171</td><td>-87.626634</td><td rowspan="2">  </td></tr>
<tr><td colspan="3">Site Description: classified as forest in the 2011 NLCD and now is classified as grassland/herbaceous in the 2016 NLCD. This image was taken by Google Earth in April 2014 with the Global Forest Change product indicating clearing 2013. Very few trees remain on the site but mixed, old growth, forest stand appears in the distance. Moderate regrowth of shrub vegetation has occurred based on satellite time lapse.</td></tr>
<tr><td></td><td>33.648482</td><td>-87.620698</td><td></td></tr>
<tr><td colspan="3">Site Description: this site is dominated by shrub land-cover as indicated in the 2016 NLCD and was cleared in 2012. This matches the pattern of several other sites that transition from forest cover in the 2011 NLCD to grassland/shrub in the 2016 NLCD. This site appears to be a bit further along in the succession of forest stand clearing with a uniform shrub layer.</td><td>  </td></tr>
</table>

LULC Change Scenarios

Land-use and land-cover can be modeled in two separate ways in hydrologic models: static and dynamic. Static land-cover maps assume no change in land use and can often oversimplify the hydrologic variation of land-cover change (Teklay et al., 2019). Static land-

cover simulations are performed in SWAT by inputting a single land-cover map and simulating it over the entire time period being tested and evaluating the SWAT output (Tamm et al., 2018). Despite static land-cover maps oversimplifying LULC change trends in hydrologic models, it uses a single climatic time series to de-trend for climate. Dynamic land-cover simulations account for land cover change over the study period by updating land-cover data at established points during the simulation, in this case, NLCD intervals (Wang et al., 2018). This project implements a blend of the two methods to model land-cover to detrend for climate (using the static run) as well as dynamically accounting for land-cover change using the 1992, 2001, 2004, 2006, 2008, 2011, 2013, and 2016 NLCDs. With the parameters that have been tested and shown to be sensitive in the watershed, the 2-year to 3-year time gap between land-cover changes in the SWAT models is sufficient for capturing the hydrologic impact of the land-cover change within the watershed as the only parameter that is largely time-dependent is GW_DELAY and is on the order of three to six weeks.

Eight different SWAT projects were created and run at a monthly timestep with all of the same adjusted parameters, soil properties, elevation data, and slope, but each with different NLCD land cover scenarios. Those scenarios were run for the respective dates the NLCD begins until December of the year prior to the next NLCD with a 3-year initialization period. For example, if the 2001 NLCD was being simulated, the warm up years would be 1998, 1999, and 2000, with the simulation beginning January 2001 and continuing until December 2003, where the 2004 NLCD would then pick up in a separate SWAT project; this is done for all NLCD scenarios 2001-2016. To de-trend for climate, a static land cover simulation was run using the land cover scenario prior to the period of study (Fig. 6). For example, the 2001 NLCD would use a static climate baseline simulation of the 1992 NLCD run through December 2003. The

differences in discharge between the 2001 and 1992 NLCD scenarios (where the overlap of the two simulations is the period of study) is the discharge change attributed to land-cover change only (LULC change contributions to discharge = dynamic LULC scenario – static climate baseline LULC scenario). Analysis of monthly discharge data and water-balance components from the 2001 through 2018 period was analyzed as well as aggregated into meteorological seasons with statistical tests applied to show discharge trends and statistical significance in discharge trends. This methodology will show if the land-cover change has had significant effects on the hydrology of the North River watershed.

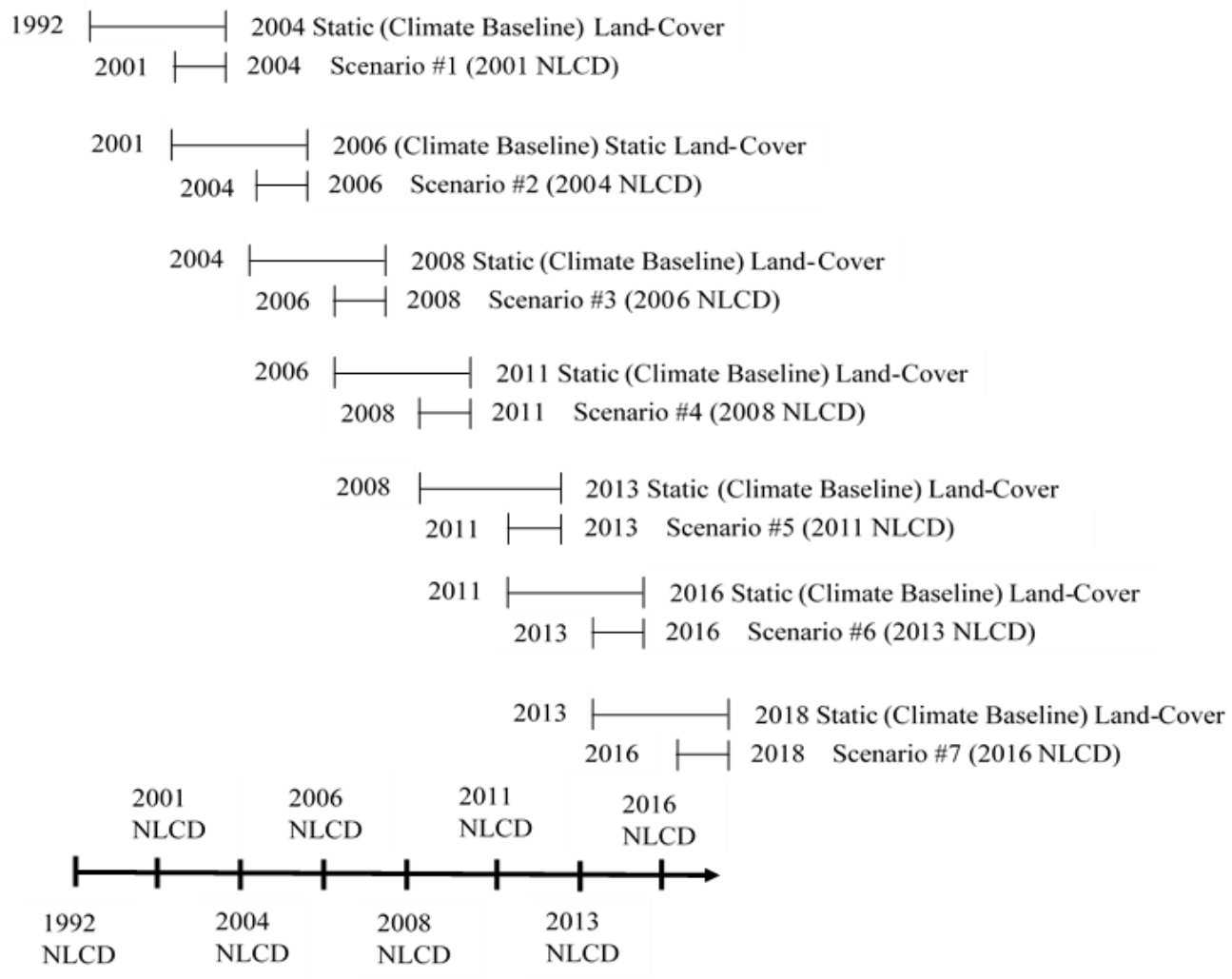

Figure 6: De-trending Process for SWAT Output. This flowchart shows the process of static and dynamic runs of LULC scenarios in the North River watershed. The static simulation is the previous land-cover scenario simulated through the entire period of interest. The static simulations set a climate baseline, which the dynamically simulated scenarios are compared against (period of overlap between two NLCD simulations), in order to isolate the land-cover change signature from climate signature in discharge.

Statistical Analyses

The assessment of the LULC change effects on the North River discharge was done on the de-trended discharge as outlined in the previous section. A cumulative distribution function (CDF) is a distribution of a random variable (*X*) and the probability that a value will fall less than or equal to *x* (Drion, 1952). The distribution function of a random variable *X* is produced by (Park, 2017):

$$F_X(x) = P(X \leq x)$$

A CDF of the monthly discharge values was produced to test for statistical significance between the NLCD scenarios run: 2001, 2004, 2006, 2008, 2011, 2013, and 2016. This CDF contained seven de-trended discharge distributions (with six transition periods) that were attributed to changes in land-cover only. A two-sample Kolmogorov-Smirnov (KS) test, a nonparametric test for one-dimensional distribution functions, was chosen to test if de-trended discharge distributions are statistically significant (Massey, 1951; MIT, 2006, *Kologorov-Smirnov test*). The H_0 that: $P_1 = P_2$ was tested using the KS-test in order to see if the two distributions are statistically the same. The KS-test statistic is (Massa, 2016):

$$D_n = \max x \, |F_{exp}(x) - F_{obs}(x)|$$

The direction of shift in means of the distribution of changes in discharge was also calculated using a Student's t-test. This is defined as the difference in two means divided by the standard error (Sokal and Rohlf, 1987; Ruxton, 2006):

$$t = \frac{\mu_1 - \mu_2}{s_p^2 \sqrt{\frac{1}{n_1} + \frac{1}{n_2}}}$$

This is defined as two sample groups (1 and 2) with the means μ, variances *s*, and sample sizes *n* of those two sample groups, in this case those are the two NLCD simulation discharges after climate de-trend. In this case, a negative test statistic would indicate that the average change in discharge increased, whereas a positive test statistic would indicate that the average change in discharge decreased from one NLCD scenario to the next (Ruxton, 2006). Once statistically significant differences in discharge years were identified, further analysis was run on those statistically significant periods, including changes in seasonal discharge by NLCD transition, and percent change of water-balance components.

In order to establish a relationship between forest coverage and discharge within the North River watershed, the purpose of this study, analysis of water-balance components produced using NLCD scenarios in SWAT were extracted. Components of the water balance variables are affected by LULC, climate, and characteristics of watershed properties such as slope, aspect, and soil characteristics (Tyagi and Rao; Accessed: 9/3/2019). Because the same elevation and soil data were used for all simulations, the only temporally changed inputs to the SWAT model were NLCD scenarios and weather data. The data extracted for the water-balance components were de-trended for climate using the same approach outlined in Figure 6, where the differences between the dynamic simulation values and static simulation values were taken to remove the climatic trends. The particular water-balance equation components analyzed were: (1) ET in mm, (2) SW in mm, (3) PERC in mm, (4) GW_RCHG in mm, (5) SURQ in mm, (6) LATQ in mm, (7) GW_Q in mm, and (8) WYLD in mm. Mango et al. (2011) analyzed these water balance components under three hypothetical deforestation LULC scenarios in order to track contributions to river discharge. Table 4 shows the many different variables SWAT uses to predict the water balance equations (Neitsch et al, 2011). ET is actual evapotranspiration

within the watershed by month in millimeters; SW is the amount of water stored in the soil profile in the watershed for a month in millimeters; PERC is water that percolates through the root zone of the soil layer in millimeters of H_2O; GW_RCHG is recharge entering the aquifers of the watershed in millimeters of H_2O; SURQ is surface runoff in the watershed per month in millimeters; LATQ is lateral flow that contributes to streamflow for the month in millimeters; GW_Q is groundwater contribution to the stream in the watershed for the month in millimeters; and WYLD is the water yield of the watershed in millimeters (SWAT Input/Output File Documentation, 2012). The percent changes between these water balance components were evaluated in order to determine how LULC change, particularly changes between forested/non-forested and vice versa, affect the hydrology of the watershed.

Table 4: SWAT water-balance components. Those tested in this study are listed with their respective variables.

Water Balance Component		Variables
ET (Penman-Monteith)	=	solar radiation, temperature, relative humidity, wind
SW	=	initial moisture, precipitation, surface runoff, ET, percolation, revap
Perc	=	SW (soil water content at any time), FC (field capacity); occurs if SW > FC
GW_RCHG	=	delay (days), peroclation, revap, base-flow
SURQ	=	rainfall, SCS curve number (function of permeability, land-use, and antecedent soil water content); occurs if rainfall > surface storage, interception, infiltration
LATQ	=	SW (excess), saturated thickness, porosity of soil (based on field capacity)
GW_Q	=	base-flow, hydraulic conductivity of aquifer, distance to main channel, water table height, recharge
WYLD	=	SURQ, LATQ, GW_Q

RESULTS

LULC Analysis and LULC Trends

The North River watershed, overwhelmingly consisting of forest, shrub/grassland, and agricultural land-cover types, has seen ~40% (~230 km^2) of its watershed suffer forest loss per the Global Forest Change product from 2001 to 2018 (Fig. 7). Using zonal statistics in ArcMap, the primary change between consecutive NLCDs (2001 through 2016), is between forest and shrubland/grassland (81% of change over study period) with secondary notable changes between forest and urban-open space as well as between forest and agriculture (Table 5). Changes between other land-cover types are negligible (~1-2% of total land within the watershed as seen in Table 5). In all of the LULC change scenarios, net change over the entire study period was small between those aforementioned categories, but gross change between individual NLCDs over the course of the study period were large, especially between forest and shrub/grassland.

The largest land-cover type by area through analysis of the NLCD LULC map, is forest cover comprised of deciduous (SCS-CN: 66), evergreen (SCS-CN: 60), and mixed forests (SCS-CN: 62) accounting for ~70% (~406 km^2) of the entire watershed with a peak of 72% (~417 km^2) in 2006 and a low of 66% (~366 km^2) in 2011, a ~35 km^2 change. The second largest land-cover type by area is the aggregated shrubland (SCS-CN: 69) and grassland (SCS-CN: 69) categories, accounting for ~15% (~86 km^2) of the watershed combined. Per the NLCD 2011 legend, shrub/scrub category is defined by shrubs (<5-meter canopy) constituting more than 20% of the

land cover. The NLCD legend notes that an area of early successional stages with young trees is classified as shrub/scrub land-cover, indicating that forest-stand regeneration after clearing or disturbance is often identified as shrub/scrub. Shrubland and grassland reached a peak coverage of ~21% (~119 km^2) in 2011 with a minimum of ~13% (~74 km^2) in 2008. The minimum spatial extent of the forest cover corresponded with a maximum extent of the shrubland/grassland category. The urban land-cover within the watershed consisted overwhelmingly of developed-open space (impervious surfaces accounting for <20% of the land cover; e.g., large-lot single-family housing units with vegetation primarily consisting of lawn grasses) and developed-low intensity (impervious surfaces accounting for 20-49% of the land-cover; e.g., single-family housing units/subdivisions) (MRLC, Accessed: June 26, 2019). Using the NLCDs from 1992-2016, urban land-cover classified as developed-open space (SCS-CN: 69) and developed-low intensity (SCS-CN: 70) account for >95% of the urban classified land-cover. Urban land-cover comprises ~4% of the watershed with watershed change amounting to less than 4 km^2. Pasture (SCS-CN: 71) and cropland (SCS-CN: 75) were aggregated into an agricultural classification and make up ~7% of the watershed. These four aggregated categories make up >95% of the watershed and were the primary categories that saw changes in spatial extent (Fig. 8). Water, barren land, and wetlands had negligible changes during the study period.

The simulated SWAT model runs were investigated under seven different past land-cover scenarios (percentages of total area and area in km^2) using NLCD products and past climate data. Six transitional periods outlined in Table 5 show the change in land-cover between the seven NLCD scenarios. With the primary focus of this study being the transition of forested land-cover to non-forested and vice versa, gross LULC change and net LULC change are shown in Table 5 categorized into forest loss and forest gain. The 2001 to 2004, 2008 to 2011, and 2013 to 2016

NLCD transitions all featured a net forest loss of 18 km^2, 29 km^2, and 9 km^2, respectively, within the North River basin. The 2006 to 2008 and the 2011 to 2013 NLCD transitions both featured a net forest gain of 3 km^2 and 36 km^2, respectively. The only transition period between two NLCD scenarios that resulted in nearly no net change in forest cover is 2004 to 2006, but it is worth noting that the overall gross forest loss and gain are substantial 44 km^2 each, which equates to nearly 15% of the watershed.

Table 5: Land Cover Change between NLCD Scenarios. Forest Loss vs Forest Gain as area (sq km.) and % of total land cover change:

	Forest Loss			Forest Gain		
2001 → 2004	Forest → Developed (Open Space)	8 km^2	9.64%	Developed (Open Space) → Forest	6 km^2	7.23%
	Forest → Shrub/Grassland	30 km^2	36.1%	Shrub/Grassland → Forest	16 km^2	19.3%
	Forest → Agriculture	4 km^2	4.82%	Agriculture → Forest	2 km^2	2.41%
		42 km^2	50.6%		24 km^2	28.9%
Other land-cover change accounting for 17 km^2 (20.5%) is between developed (open space), shrub/grassland, and agriculture.						
2004 → 2006	Forest → Developed (Open Space)	8 km^2	7.62%	Developed (Open Space) → Forest	8 km^2	7.62%
	Forest → Shrub/Grassland	34 km^2	32.4%	Shrub/Grassland → Forest	32 km^2	30.5%
	Forest → Agriculture	2 km^2	1.90%	Agriculture → Forest	4 km^2	3.81%
		44 km^2	41.9%		44 km^2	41.9%
Other land-cover change accounting for 17 km^2 (16.2%) is between developed (open space), shrub/grassland, and agriculture.						
2006 → 2008	Forest → Developed (Open Space)	5 km^2	5.68%	Developed (Open Space) → Forest	5 km^2	5.68%
	Forest → Shrub/Grassland	30 km^2	34.1%	Shrub/Grassland → Forest	33 km^2	37.5%
	Forest → Agriculture	1 km^2	1.14%	Agriculture → Forest	1 km^2	1.14%
		36 km^2	40.9%		39 km^2	44.3%
Other land-cover change accounting for 13 km^2 (14.8%) is between developed (open space), shrub/grassland, and agriculture.						

Table 5 Cont.: Land Cover Change between NLCD Scenarios. Forest Loss vs Forest Gain as area (sq km.) and % of total land cover change:

2008 → 2011	Forest → Developed (Open Space)	6 km^2	4.84%	Developed (Open Space) → Forest	8 km^2	6.45%
	Forest → Shrub/Grassland	60 km^2	48.39%	Shrub/Grassland → Forest	27 km^2	21.77%
	Forest → Agriculture	2 km^2	1.61%	Agriculture → Forest	4 km^2	3.23%
		68 km^2	54.84%		39 km^2	31.45%
Other land-cover change accounting for 16 km^2 (12.9%) is between developed (open space), shrub/grassland, and agriculture.						
2011 → 2013	Forest → Developed (Open Space)	5 km^2	4.24%	Developed (Open Space) → Forest	4 km^2	3.39%
	Forest → Shrub/Grassland	29 km^2	24.6%	Shrub/Grassland → Forest	64 km^2	54.2%
	Forest → Agriculture	1 km^2	0.85%	Agriculture → Forest	3 km^2	2.54%
		35 km^2	29.66%		71 km^2	60.17%
Other land-cover change accounting for 13 km^2 (11.0%) is between developed (open space), shrub/grassland, and agriculture.						
2013 → 2016	Forest → Developed (Open Space)	5 km^2	9.80%	Developed (Open Space) → Forest	4 km^2	12.90%
	Forest → Shrub/Grassland	19 km^2	37.3%	Shrub/Grassland → Forest	11 km^2	21.57%
	Forest → Agriculture	2 km^2	3.92%	Agriculture → Forest	2 km^2	3.92%
		26 km^2	51.0%		17 km^2	38.4%
Other land-cover change accounting for 4 km^2 (7.84%) is between developed (open space), shrub/grassland, and agriculture.						

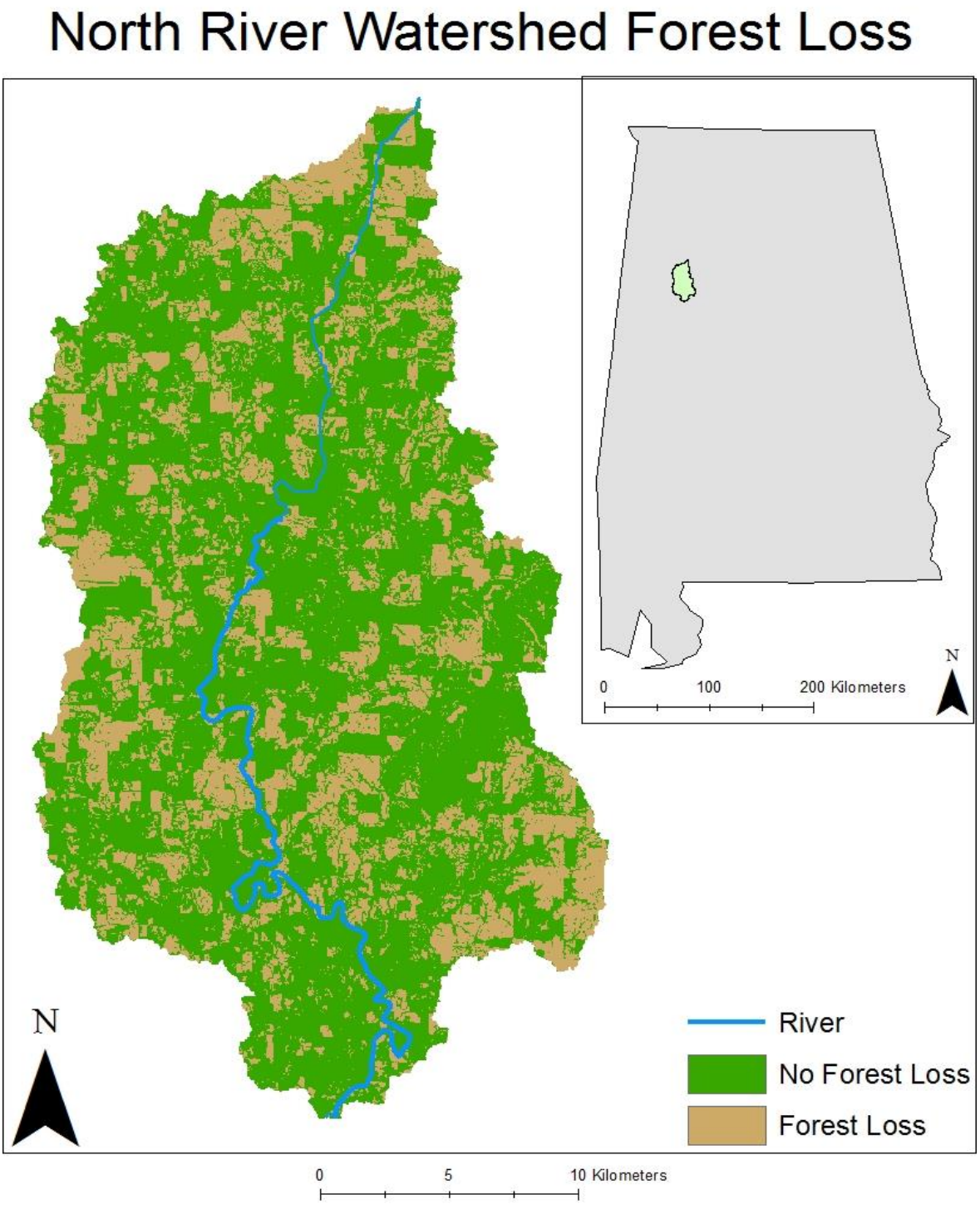

Figure 7: Map of Total Forest Loss (2001 to 2018). Thematic map of the North River watershed produced from the Global Forest Change Product. This map shows the regions of the watershed that has seen gross forest loss between 2001 and 2018. This map does not include net forest lost (forest gain combined with forest loss).

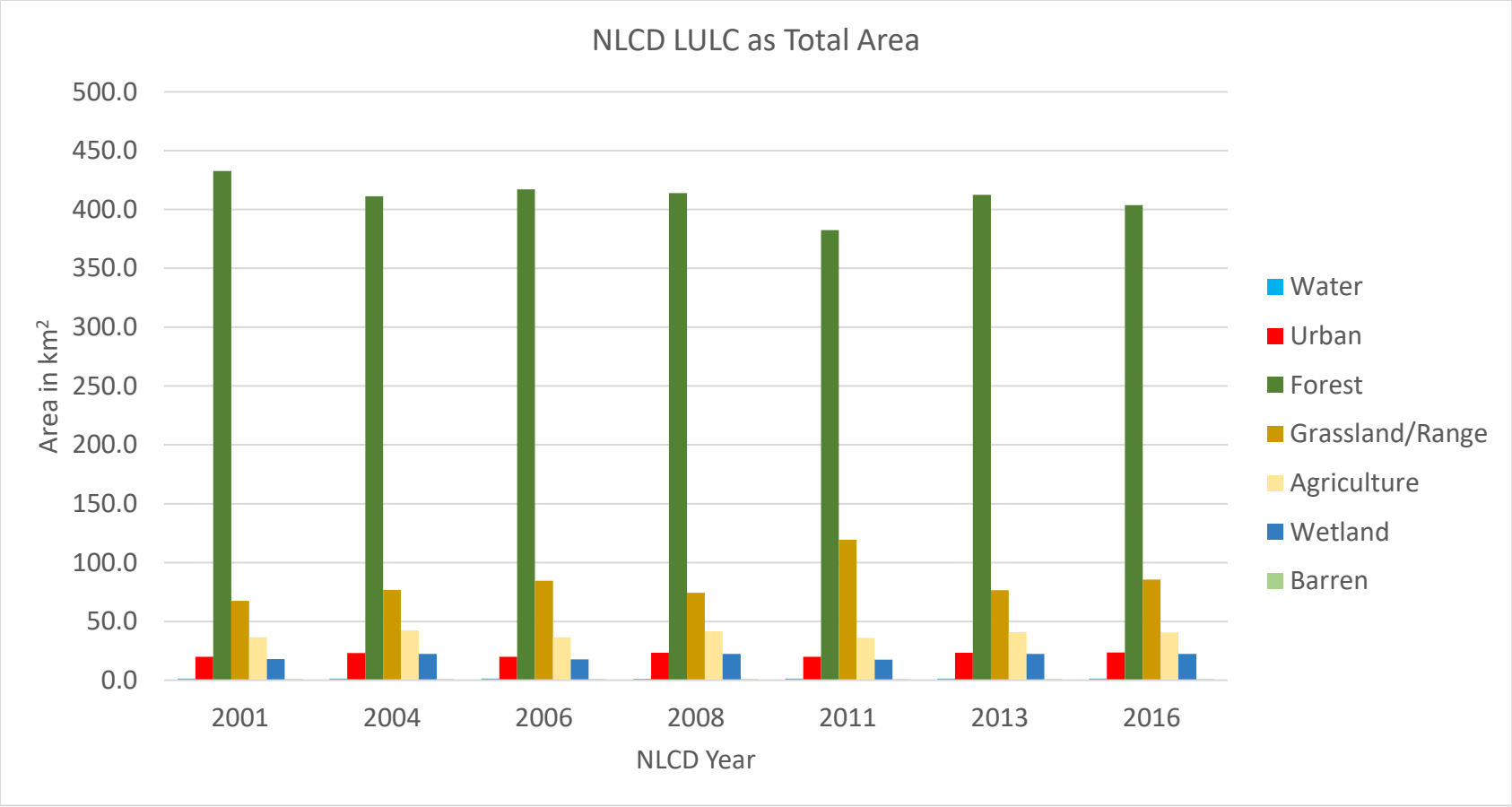

Figure 8: LULC as Total Area of Basin. Land-cover broken down into seven aggregated categories: water, urban, forest, grassland/range, agriculture, wetland, and barren. Fluctuations in spatial coverage of LULC is noted by each NLCD. Large spatial coverage of forest peaks in the 2001 NLCD with smallest spatial coverage in the 2011 NLCD. It is also noted that the smallest and largest cover of shrub/grassland coincide with largest and smallest coverage of forest LULC, respectively.

Hydrologic Changes

As the primary goal of this study is to assess the effect of LULC change on discharge from the North River, monthly discharge values from SWAT simulations were de-trended using the method outlined in Figure 6 (de-trended discharge = dynamic run – static run) and plotted on a cumulative distribution function (CDF) for each NLCD simulation (Fig. 9). Over the entire study period, from 2001 to 2018, there was a non-statistically significant declining trend in discharge, which is shown in Figure 9 by the overall shifting of the CDFs to the left of zero. When assessing the statistical differences between the seven NLCD scenarios, the KS-test revealed statistical significance between three of the six land-cover transition periods between NLCDs. Table 6 shows the periods of transition of land-cover by NLCD years with statistically significant years noted. Two of the three transitions marked as having significant changes in discharge had the largest transition from: (1) forested to non-forested land-cover (2008 to 2011) or (2) non-forested to forested land-cover (2011 to 2013). In order to further isolate LULC change as a primary driver of the change in discharge, analysis of water-balance components was done to extract percent changes from de-trended data of variables that contribute to river discharge (Fig. 10). With the largest shift from forest to non-forest in the 2008 to 2011 NLCD scenario as shown in Table 5, the watershed experienced a sizeable reduction in water stored in the soil profile (~ -7%) and ground water contribution to streamflow (~ -5%) with a large increase in surface runoff (~ +10%), groundwater percolation through the soil profile (~ +4%), and lateral flow into the river channel (~ +3%). On the other end of scenarios, the largest shift from non-forested land-cover to forested land-cover between the 2011 and 2013 NLCD scenarios (Table 5) produced reduced surface runoff (~ -4%) and reduced lateral flow to the river channel (~ -2%) with an increase in evapotranspiration. The pattern of reduced evapotranspiration,

increased surface water runoff, and increased percolation from the soil into ground-water was noted for other NLCD years with less pervasive forest conversion to non-forested cover (2001 to 2004 and 2013 to 2016) at a lesser magnitude.

Table 6: Discharge change associated with land-cover change. This is NLCD year simulations in ArcSWAT. Kolomorgov-Smirnov test (2-sided) results are shown along with the direction of change.

Cumulative Distribution Function			Asymptotic Sig. (2-sided test)	Test Statistic (Directionality)
2001	→	2004	0.106	-0.047
2004	→	2006	0.002*	4.458
2006	→	2008	0.978	-0.218
2008	→	2011	0.007*	-3.983
2011	→	2013	0.000*	5.69
2013	→	2016	0.504	-1.332

* Indicates statistical significance at a 0.05 level.

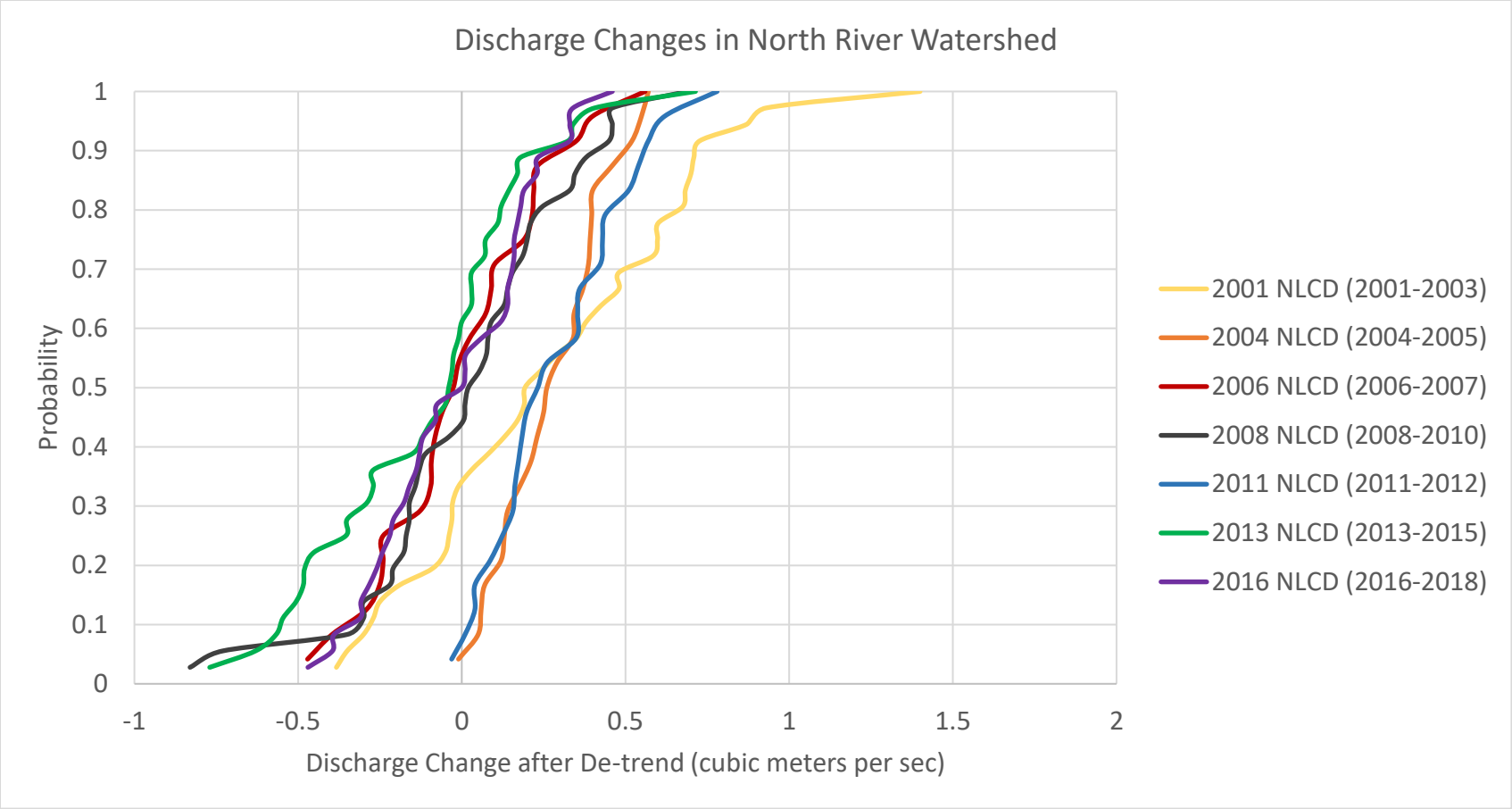

Figure 9: Discharge CDFs of NLCD Scenarios. The cumulative distribution function (CDF) of de-trended changes in discharge produced from SWAT simulations. The large shifts in mean are noted for the statistically significant changes in NLCD as listed in Table 6.

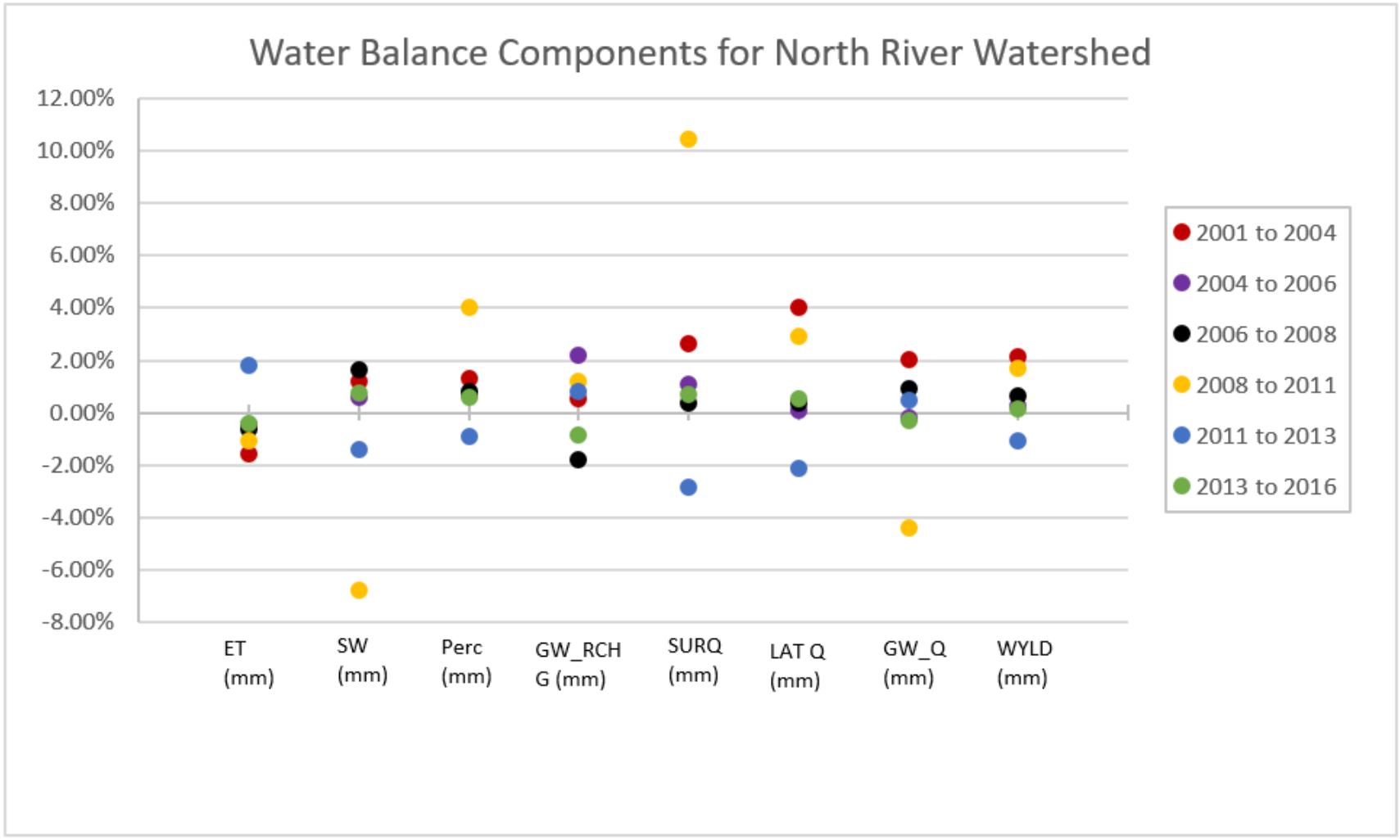

Figure 10: Percent Change in Water Balance Components. This is for six different NLCD transition periods from 2001 to 2016 within the North River watershed.

The trend of decreasing discharge is noted in Figure 9, where the latter CDFs are falling behind the former CDFs. Figure 11 contains the change in monthly discharge after removing the climate signal. Notable change in monthly discharge over the entire study period was negligible. 2008 to 2011 LULC change scenario had monthly discharge increase due to the extensive forest removal and subsequent increase in water yield attributed to less evapotranspiration. Other scenarios, such as 2001 NLCD and 2004 NLCD, show a majority of monthly discharge amounts that increased. The 1992 to 2001 NLCD saw a forest decrease much like the 2008 to 2011 NLCD, indicating that forest removal is a reliable indicator of increasing discharge amounts. A monthly flow rate chart was also produced using both the regular monthly discharges and the de-trended discharges on order to highlight monthly and seasonal changes in discharge (Fig. 12). In the case of years with forest loss (2001-2004 and 2008-2011), there was a consistent a net increase in discharge related to LULC change. With NLCD scenarios involving forest gains (2006-2008 and 2011-2013), decreases in net discharge were shown in later summer months through fall and early winter. In one NLCD case (2004 to 2006), monthly discharge was quite variable with summer discharge values reduced from the previous land-cover scenario with an increase from previous land-cover scenarios in the late fall and winter months. To further track seasonal changes in discharge, a chart tracking changes in discharge by meteorological seasons through NLCD scenarios are shown in Figure 13. When looking at the three statistically significant NLCD LULC changes, the seasonal de-trended discharges highlight differences when compared to non-significant LULC change scenarios. Starting with 2004 to 2006, summer discharge decreased markedly (on the order of 0.1-0.5 m^3/s) under a different LULC scenario that featured no net change in LULC. For 2008 to 2011, seasonal discharge increased uniformly

with only one fall monthly value having a decrease in discharge. 2011 to 2013 saw a large range of changes in discharge, particularly during the fall months.

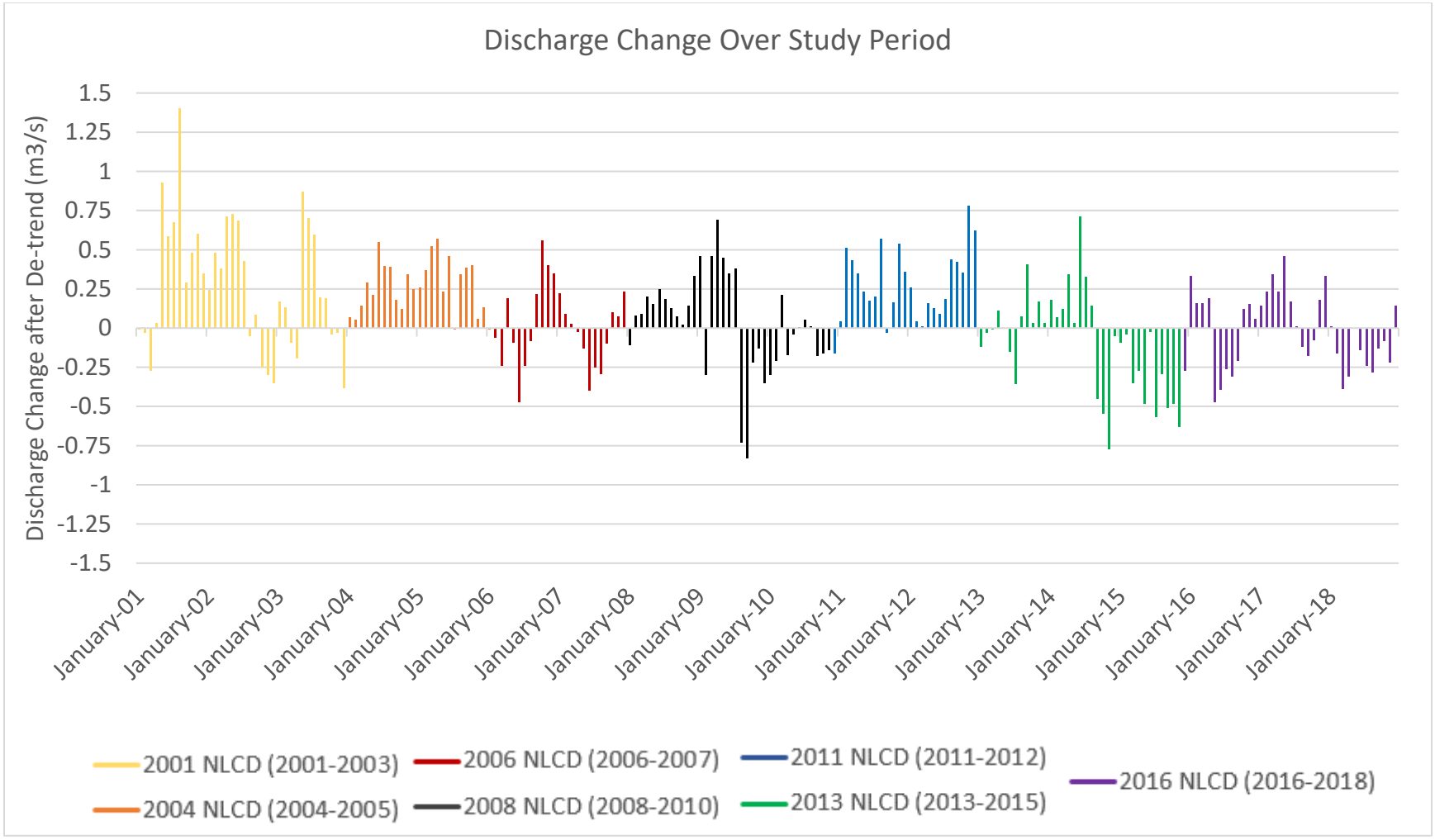

Figure 11: Monthly Discharge Changes over Study Period. Changes in monthly discharge between NLCD scenarios due to LULC change after climatic signal removal. Each NLCD scenario is colored differently. Over the entire study period, there has been minimal change in discharge amounts, but large differences are noted within change scenario changes.

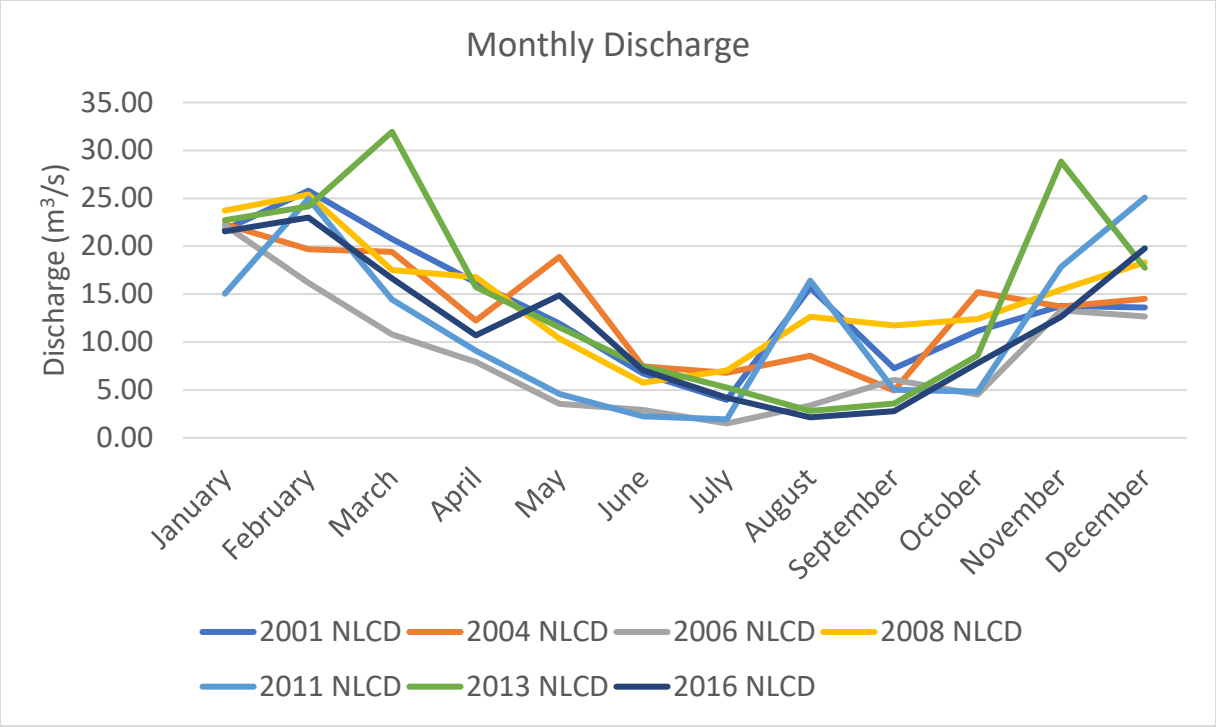

Figure 12a: Monthly Flow Rate Chart (no climate de-trend). This is each NLCD scenario and is not climate de-trended. Note the seasonal changes in discharge.

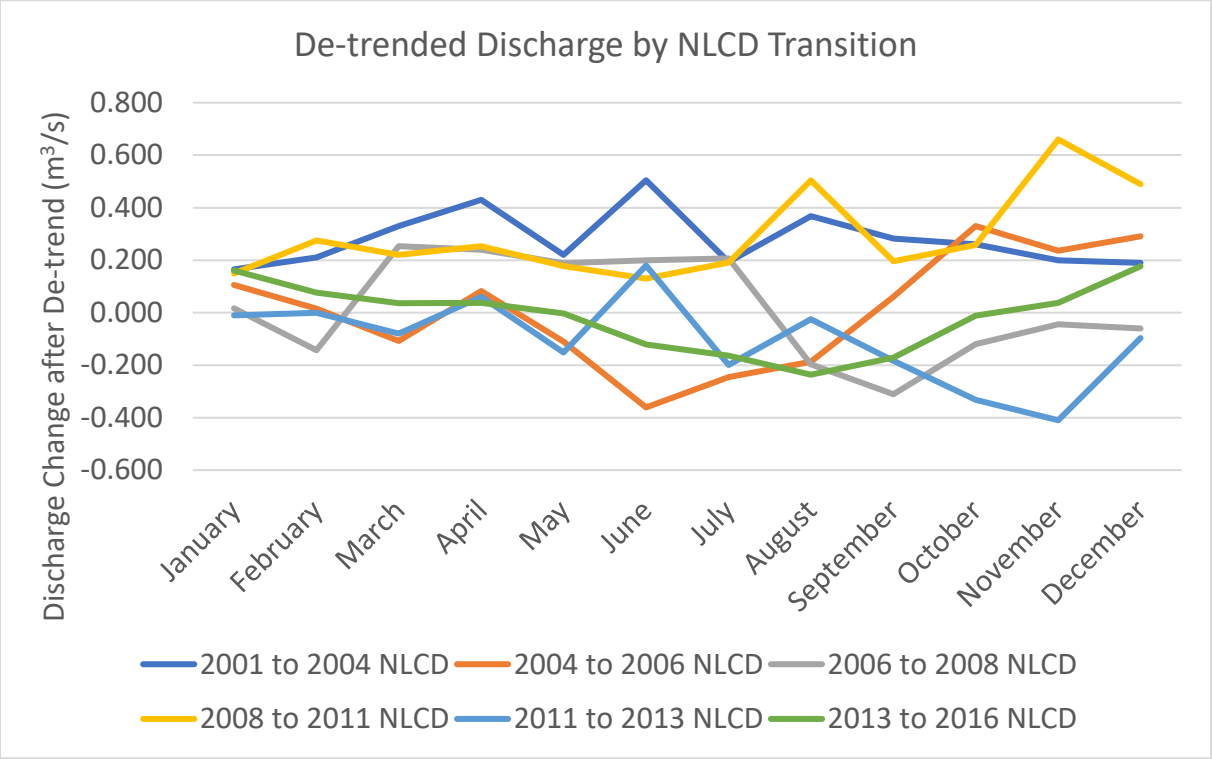

Figure 12b: Monthly Flow Rate Change by NLCD Transition (with de-trend). These are changes between NLCD periods attributable to LULC change solely.

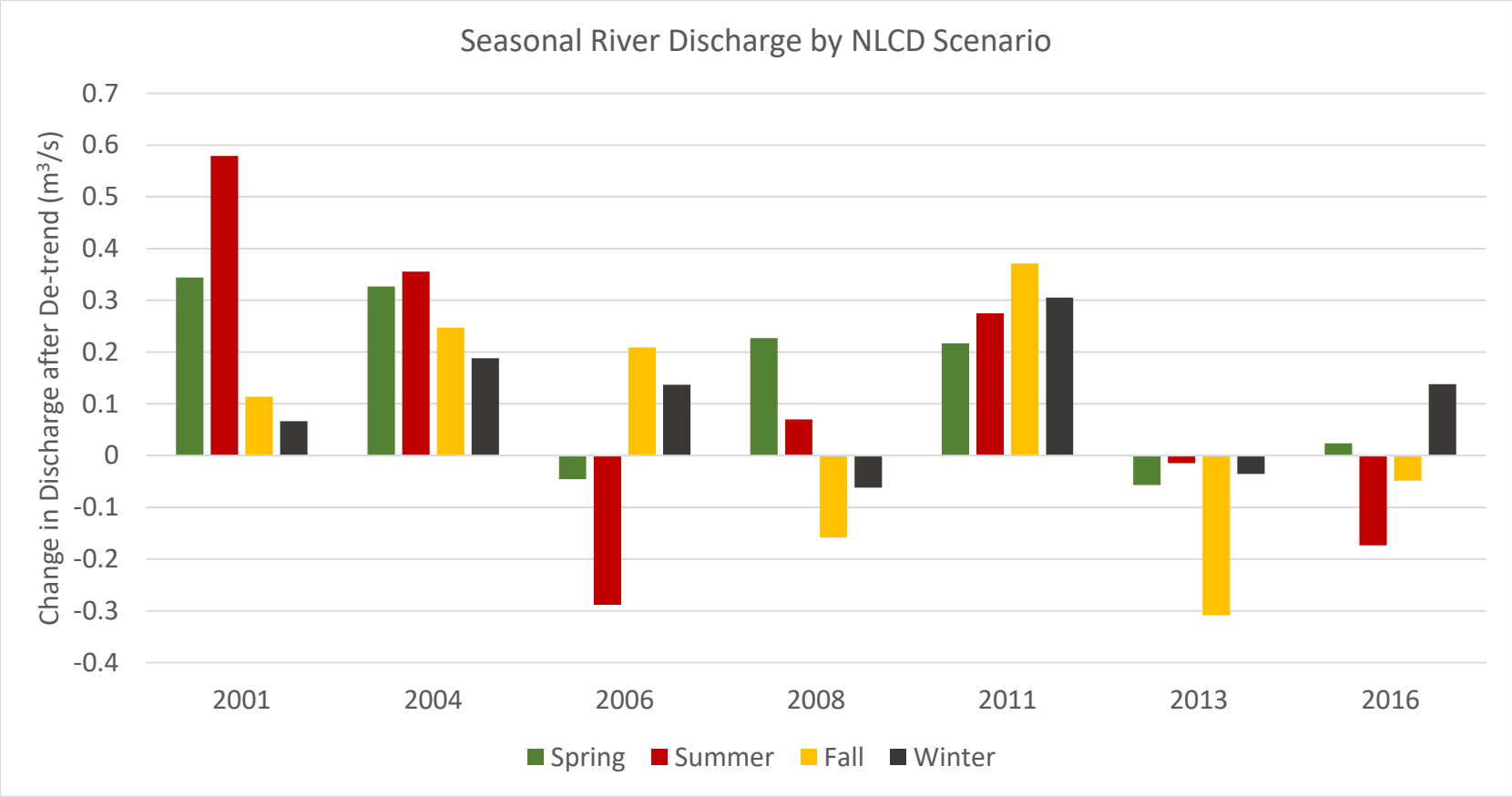

Figure 13: Chart of Seasonal Discharge Changes between NLCD Scenarios. Monthly values are aggregated into meteorological seasons and then averaged for the NLCD scenario in order to note seasonal discharge for LULC change. Noted are the large seasonal changes in discharge between 2004 to 2006, 2008 to 2011, and 2011 to 2013 NLCD change scenarios, which all were statistically significant changes.

DISCUSSION

LULC Analysis and Trends

The trend noted for forest and non-forest conversions in the North River watershed match other trends throughout the Southeast. The North River watershed is located in a complex area of change with the hallmark signatures of intensive forestry for the primary purpose of logging and harvest. The recurrent transitions of forest to shrub/grassland/open developed stages or the reversal of that sequence, for the purpose of timber harvesting or stand regeneration, accounted for >80% of the LULC change in every NLCD change scenario. As noted by Drummond et al. (2015), cyclical forest replacement with a trajectory from mature forest stand to transitional grassland and shrubland covers are due to intensive plantation silviculture. The LULC change in the North River is typical of Southeast Coastal Plain; the majority of forest removal is caused by plantation silviculture with a recurring land-cover trajectory (Drummond et al, 2015). The cleared forest stands are on short rotation (10-12 years with a maximum of 15 years) with a brief disturbed/transition state characterized by shrub/grassland presence prior to forest growth and classification as forest in NLCD products (Yang et al., 2018). This matches the findings in the site verification done to selected 2011/2016 NLCD classifications and changes noted in Table 3, where land-cover classified as forest was recently cleared and patches classified as shrub/scrub were now young-growth trees. These networks of patches are shown in thematic forest loss (forest to shrub/grassland/developed open-space) or forest gain (shrub/grassland/developed open space) maps for NLCD transitions in Figure 14 through Figure 19. Urban growth was minimal

within the watershed, with small fluctuations in agriculture and pasture coverage (< 20% of NLCD change). Nearly 40% of the watershed has had forest clearing (Fig. 7) through the study period (2001 to 2018), with noted forest regrowth after exhibiting the cyclical transition to developed-open space or grassland/shrubland in LULC scenarios. This indicates that LULC involving forestry and forest management is ongoing within the watershed. With the Department of Agricultural Economic and Rural Sociology in Auburn University (2013) indicating intensive forestry as an important component of the economy within the North River watershed and the Southeastern U.S., future LULC in forested regions will be shaped by economic trends of commercial logging.

Hydrologic Changes

The effects of LULC change on streamflow in the North River watershed were derived from comparisons between transitions from past land-cover scenarios produced by the NLCD. Two of the largest changes in land-cover resulted in statistically significant changes in the distribution of de-trended discharge, meaning the loss or recovery of forested area accounting for >5% of the watershed resulted in fundamental changes in the water balance. The 2011 to 2013 scenario, which saw a net forest-cover increase of 6-7% (36 km^2), yielded an inverse relationship between base-flow/surface runoff and evapotranspiration. The increase in forest coverage within the watershed resulted in increasing evapotranspiration rates which caused soil-water content, percolation into the shallow aquifer, surface runoff, and base flow to decrease. This is strongly noted in the monthly flow rate as discharge was reduced during later summer months through fall and early winter (Fig. 12). The decrease in discharge seen during later summer and early fall months is likely attributed to increased ET from more forest cover. The decrease in discharge in fall and early winter, where surface runoff becomes the larger contributor to streamflow versus

base flow in the summer, is likely from reduced surface runoff from increased vegetation. Forest canopy and underbrush increases interception of precipitation, thus reducing the velocity of precipitation, in turn reducing runoff velocity and well-established root structures allow for infiltration into the soil (Arceo et al., 2018). Because the difference between precipitation and evapotranspiration determines the water yield, the change in land-cover (increase in forest cover) is directly attributable to the decrease in water yield (Ward et al., 2018). These results are consistent with other findings that afforestation reduces water yield, especially when forest coverage already constitutes the majority of LULC. The shift in land-cover brought about significant changes in the form of decreased discharge in the North River watershed during the aforementioned time frame.

Between 2008 and 2011, there was a decrease in forest cover of 5-6% (29 km^2) which also matched the inverse relationship between base-flow/surface runoff and evapotranspiration as seen in 2011-2013. Decreased evapotranspiration resulted in increased base-flow caused by increased percolation. Reduction in forest cover also resulted in large increases in surface runoff (>10% over previous land-cover scenarios) and decreases in soil-water content (Githui et al., 2010). Surface runoff in SWAT is determined by the SCS curve number (a function of antecedent soil water conditions, land-use, and permeability to estimate an infiltration rate) and any water that does not infiltrate into the soil profile becomes runoff. Despite a net decrease in soil-water content, the infiltration rates of the non-forested LULC resulted in greater surface runoff, which is the largest takeaway from this. Groundwater recharge increased in conjunction with percolation, but there was a significant reduction in groundwater flow, which can potentially be attributed to a lag related to the previous NLCD (2006-2008) reduction in groundwater recharge caused by large forest loss in headwater retention areas (Fig. 16).

Reinhardt-Imjela et al. (2018) have shown that vegetation in headwater regions plays a pivotal role in flood-runoff formation and capture/retention of water within the system. Gong et al. (2012) showed that land-cover and precipitation play influential roles in determining groundwater recharge and the delay related to water-table heights. Combining the effects of declining evapotranspiration and large increases in percolation, base-flow, and surface runoff, a net positive increase in water yield occurred. Figure 12 shows the monthly changes in discharge with respect to each month. For the 2008 to 2011 LULC change scenario, monthly discharge for every month exemplified a net increase driven by forest removal. This change was most noted during the late summer, fall, and early winter months. The peak seen during the late summer months is likely base flow (due to the increase in percolation/reduction in ET from vegetation removal) while the peak seen during fall and winter months is more attributed to surface runoff from less vegetative cover. The implication of removing forest cover is shown greatly in the surface-runoff increases, which can contribute to flashier hydrographs, ones where the peak flows are more amplified and lag time is shorter resulting in greater flood risks during heavy rainfalls (Reinhardt-Imjela et al., 2018). It is important to understand the interactive hydrology within the North River watershed, where runoff volume and water yield have a negative correlation with forest cover. With dynamic and rapid changes in forest cover within a watershed vital to reservoir supply, large surface runoff changes and subsequent water yield changes triggered by forest removal can be used to model future scenarios to ensure steady and consistent supply to a public water source.

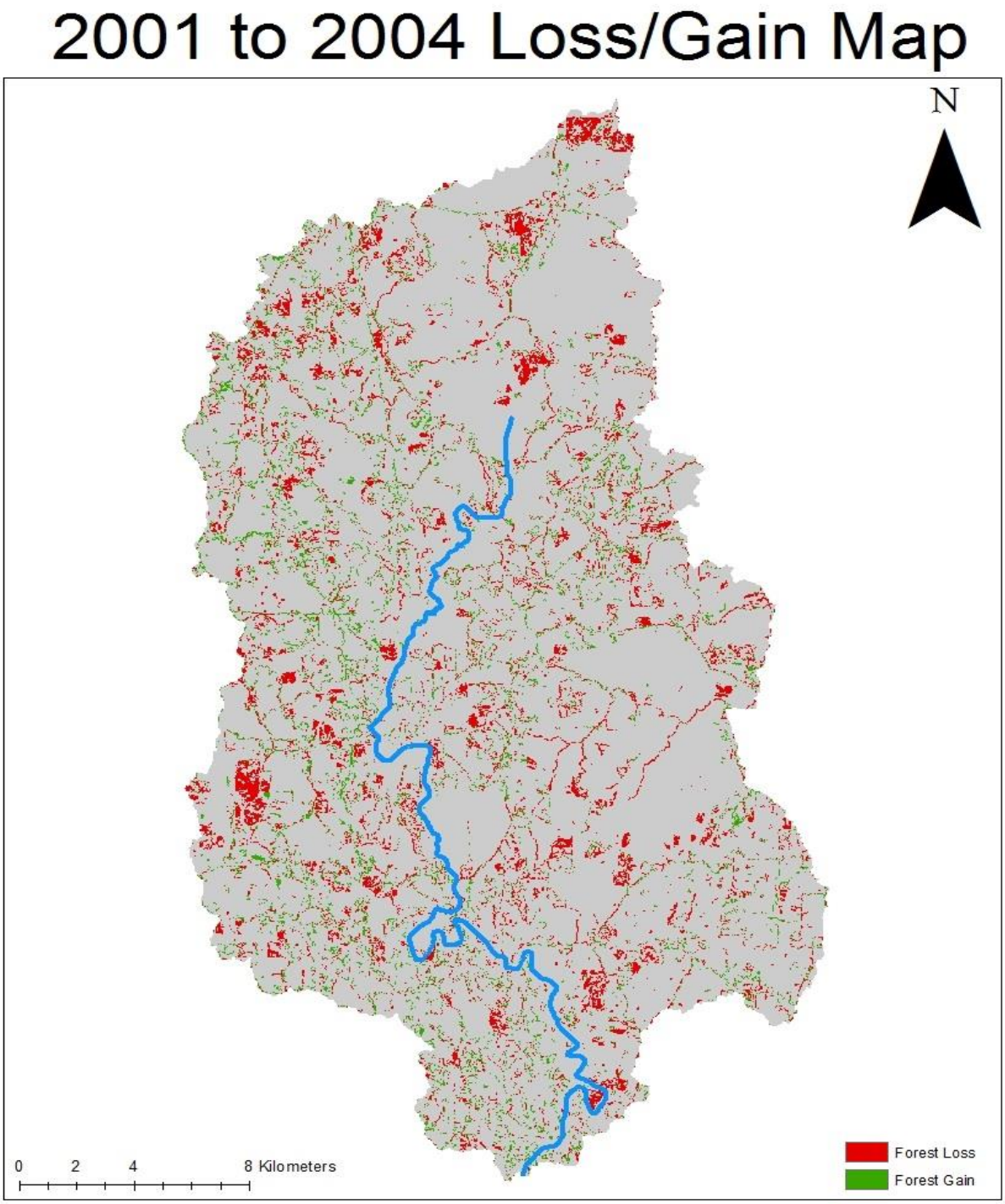

Figure 14: 2001 to 2004 Change Map. Land-cover transition maps outline the change in forest cover (either gained or lost) between the 2001 and 2004 NLCD. The red indicates forest lost and green indicates forest gain between the years listed at the top of the map. Shown are the large clear-cut patches associated with intensive forestry (red) or green associated with regrowth associated with succession in forest plantations used for industry.

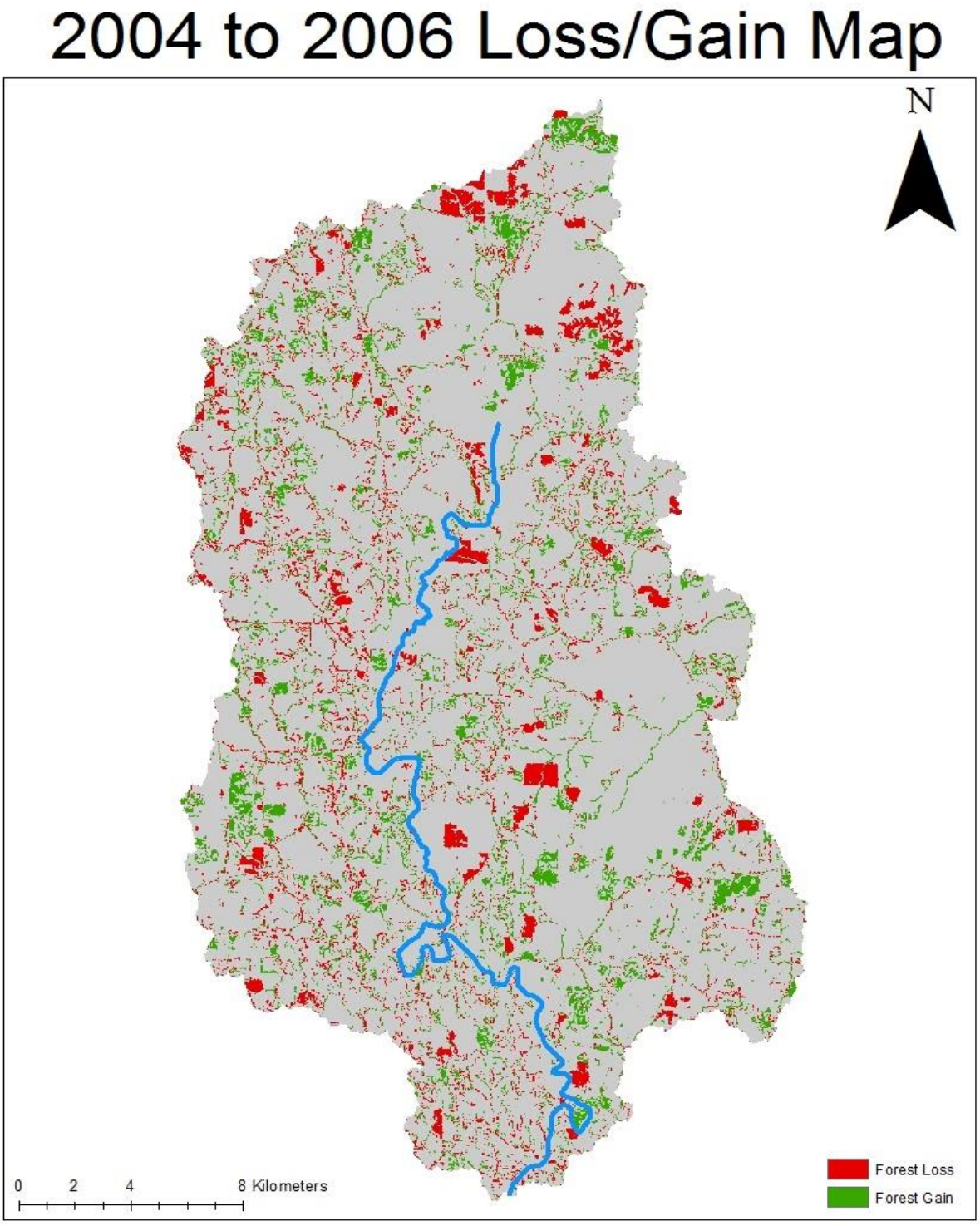

Figure 15: 2004 to 2006 Change Map. Land-cover transition maps outline the change in forest cover (either gained or lost) between the 2004 and 2006 NLCD. The red indicates forest lost and green indicates forest gain between the years listed at the top of the map. Shown are the large clear-cut patches associated with intensive forestry (red) or green associated with regrowth associated with succession in forest plantations used for industry.

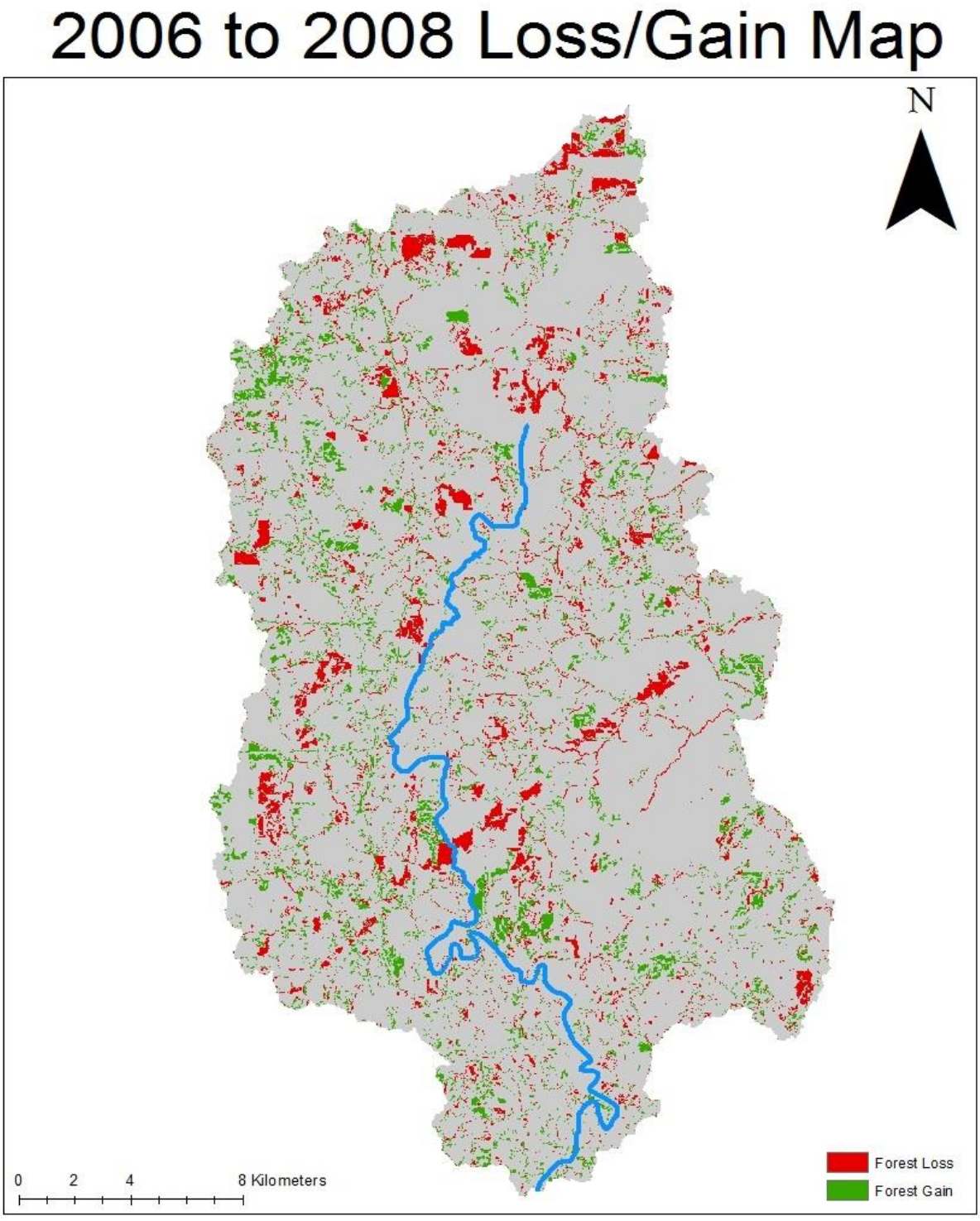

Figure 16: 2006 to 2008 Change Map. Land-cover transition maps outline the change in forest cover (either gained or lost) between the 2006 and 2008 NLCD. The red indicates forest lost and green indicates forest gain between the years listed at the top of the map. Shown are the large clear-cut patches associated with intensive forestry (red) or green associated with regrowth associated with succession in forest plantations used for industry.

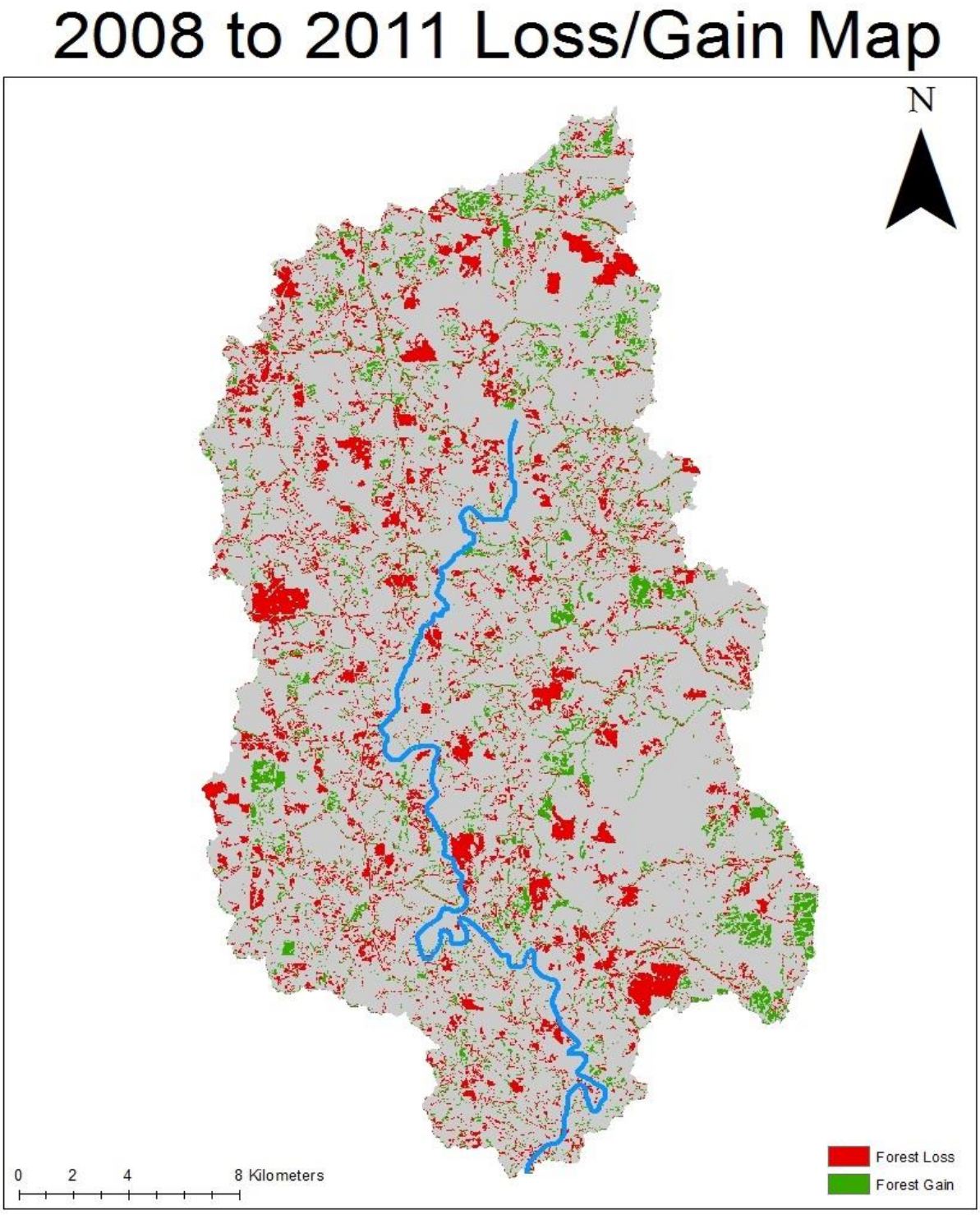

Figure 17: 2008 to 2011 Change Map. Land-cover transition maps outline the change in forest cover (either gained or lost) between the 2008 and 2011 NLCD. The red indicates forest lost and green indicates forest gain between the years listed at the top of the map. Shown are the large clear-cut patches associated with intensive forestry (red) or green associated with regrowth associated with succession in forest plantations used for industry.

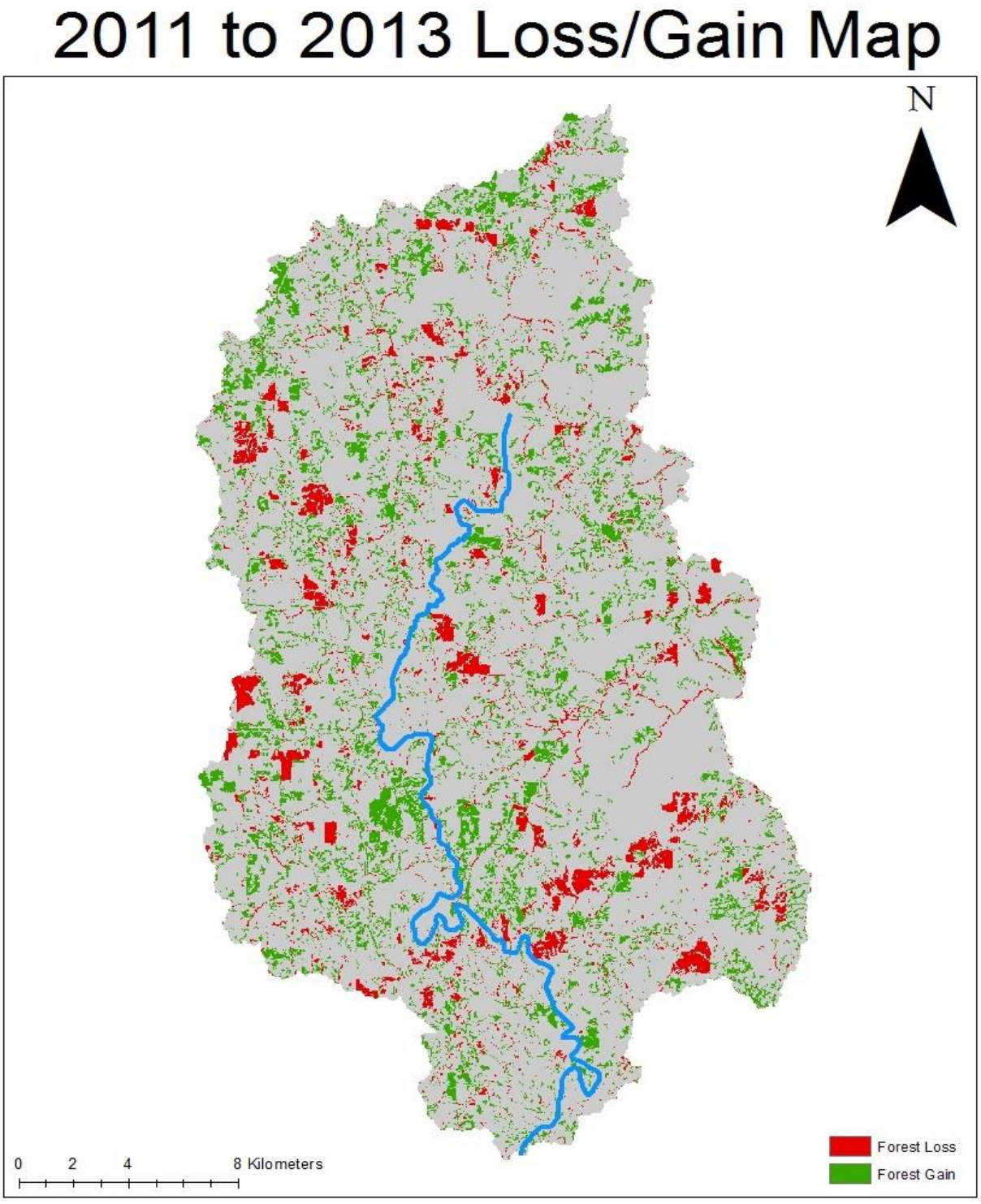

Figure 18: 2011 to 2013 Change Map. Land-cover transition maps outline the change in forest cover (either gained or lost) between the 2011 and 2013 NLCD. The red indicates forest lost and green indicates forest gain between the years listed at the top of the map. Shown are the large clear-cut patches associated with intensive forestry (red) or green associated with regrowth associated with succession in forest plantations used for industry.

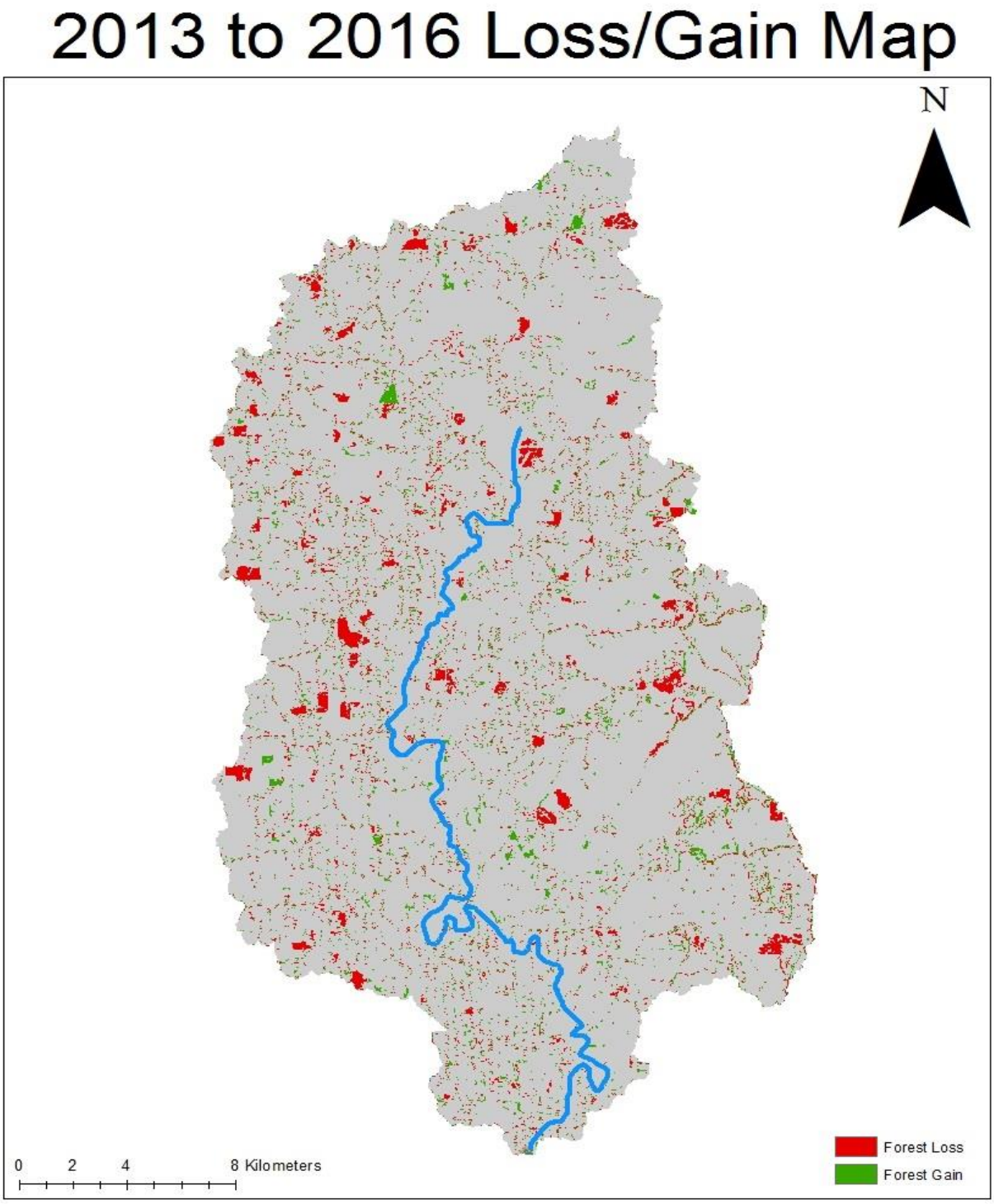

Figure 19: 2013 to 2016 Change Map. Six land-cover transition maps outline the change in forest cover (either gained or lost) between the 2013 and 2016 NLCD. The red indicates forest lost and green indicates forest gain between the years listed at the top of the map. Shown are the large clear-cut patches associated with intensive forestry (red) or green associated with regrowth associated with succession in forest plantations used for industry.

As seen in Table 6, the 2004 to 2006 LULC change was the only other LULC change period that resulted in a statistically significant change in discharge despite having a net-zero change in forest loss. With the other two statistically significant scenarios featuring the greatest amount of forest loss (2008 to 2011 at ~5-6% of the watershed) and the greatest amount of forest gain (2011 to 2013 at ~6-7% of the watershed), the relationship between evapotranspiration, surface runoff, soil moisture content, and water yield have clear trends under certain LULC change scenarios. The 2004 to 2006 LULC change scenario results in large seasonal changes as shown in Fig. 8 and Fig. 9. The large decrease in summer discharge and large increase in fall discharge between 2004 and 2006 attributed to LULC change is likely the driver for the statistically significant results. Seasonal CDFs of de-trended discharges lead to a few hypotheses regarding the specific LULC driver that modifies the hydrologic components. As LULC is the only change between scenarios with other model inputs remaining constant, two potential LULC change hypotheses are: (1) distance of forest clearings or regrowth patches in relation to main stream channel result in fundamental water-balance changes of the watershed or (2) patch size of forest clearing or forest regrowth and ratio between the two result in changes of the water-balance of the watershed.

With the distance of LULC change patch to stream channel hypothesis, it is noted by Shrestha (2019), that smaller catchments and headwater streams are more sensitive to LULC change with net changes in discharge being significantly larger in magnitude for smaller streams and headwater tributaries. Forest growth in headwaters lowers water yield by increasing infiltration into the soil and uptake by deep rooted trees with loss through evapotranspiration and overall net reduction in soil moisture content (Wahren et al., 2012). Wang et al. (2018) also notes that headwaters of watersheds are vital for groundwater recharge and streamflow. Using a

proximity analysis in GIS with analysis of patch distances to stream channel, a simple t-test can be performed to see if distances to stream channel of forest removal or forest gain patches are statistically different. Patch size of forest regeneration or clearing has shown that larger LULC change patches attributed to forest growth or forest removal have greater effects on discharge. As noted by Ide et al. (2013), greater reductions in soil moisture storage and larger areas with less tree interception attributed to forest clear-cuts will have subsequent greater surface-water and groundwater modulations caused by intensive forestry. The positive relationship between area of intensive forestry and surface runoff rates with earlier occurrence of peak flows is shown by Ide et al. (2013). Through the use polygon calculations, the area of patch sizes of both forest gain and loss can be quantified. A weighted overlay analysis within ArcGIS can be performed on the patch sizes, where greater consideration is given to larger patch sizes, as their effect on hydrology is magnified. Combining both the statistical tests for distance to stream channel and patch size analysis, statistical significance of both can be assessed. In addition, hypothetical LULC scenarios in different parts of the watershed and comparing the hydrologic response with other LULC change scenarios can allow for further testing size and location of forest loss or gain within the watershed and the water-balance response. With the summer discharge of the 2004 to 2006 LULC change seeing such a large decrease over the previous LULC scenario and the hydrology of the watershed favoring base-flow as the primary source of streamflow for summer months, location and size of the LULC change patches are likely drivers of hydrologic changes that will need further testing.

In some of the years where the changes in discharge were not statistically significant, results mimicked previous findings in other NLCD scenarios. For the 2006 to 2008 LULC scenario, there was a small net increase in forest cover. Groundwater recharge had the largest

percent change between the 2006 and 2008 land-cover scenarios, likely as a result of the distribution and size of forest loss and gain patches, similar to the 2004 and 2006 LULC change scenario. Further testing, similar to the 2004 to 2006 suggestions, may be required to see what trends are reflected in the distance to stream channel and size analysis of the forest gain or loss patches. Combining analysis of the patch locations and sizes along with individual water-balance components (in this case, the increase in groundwater recharge) will give a clearer idea of the distribution and trends in LULC change with the goal of increasing groundwater recharge and water yield within a watershed. The 2001 to 2004 scenario featured the second largest forest-cover removal, which reflected the reduction in evapotranspiration, increase in soil-water content and percolation into the groundwater caused by less vegetation using available soil-water. Surface runoff, base-flow, and percolation all increased as a result of increased soil water content, which lead to an increase in water yield from the watershed. As noted in the 2004 to 2006 and 2006 to 2008 NLCD LULC change scenarios, further analysis of distribution and size of patches will further clarify how these influence water balance components. The only other LULC change scenario was between 2013 and 2016, where water balance components fluctuated minimally (<1% change) and net LULC change was less than 2% of the watershed.

Implications

From this study, the decrease in water yield (and subsequently discharge) following LULC change involving forest regrowth periods can be attributed to increasing ET resulting in decreases in SURQ, PERC, and LATQ. Under increased forest coverage, there exists reductions in recharge to surface reservoirs through lower surface runoff, lower lateral flow contributions, and overall lower total water yield of the watershed. Changing climatic conditions with anthropogenic climate change, particularly increases in drought, can severely impact water-

security, defined as: the sustainable use and protection of access to water for the service of humans and the ecosystem and to protect against water-related hazards (Wheater and Gober, 2015). Water for urban municipalities, who primarily get their water resources through surface-water reservoirs and groundwater (Craig et al., 2019), are at greatest risk. Per Roundy and Yuan (2015), drought is the primary economic hardship for the Southeast U.S., particularly agriculture. With intensifying cycles of drought expected through 2050, the economy of the Southeast U.S. in terms of water security for agriculture and urban growth will become increasingly susceptible (Craig et al., 2019). The concern among citizens of the Southeastern U.S. with regards to water security is no clearer than in the Tri-State water wars, a contested battle over the control of water between the Alabama-Coosa-Tallapoosa river basin and the Chattahoochee-Apalachicola-Flint river basin. Within the state of Alabama, there is no statewide water management plan, which weakens attempts to litigate water uses with other states (Chitwood, 2016). Forest removal temporarily increases water yield through replacement of fast-growing, newly matured forest stands with shrub and/or grassland (LULC with significantly fewer trees). With the cycle of tree regeneration amongst stands several years after clearing, reductions in water yield become apparent. These clear increases and decreases in water yield, caused by LULC change, can impact water resources that continually face greater supply issues, not only in the Southeastern U.S. as discussed, but across other parts of the world. With the need for watershed policies within the state of Alabama and the unknown effects of LULC change on water yield, this study solidifies conceptual findings of LULC change effects on hydrology.

This study focused on a rural, highly forested watershed subjected to intensive plantation forestry. With many rivers in the Southeast U.S. and other parts of the country and world having LULC change that affect water security, the SWAT modelling of realistic LULC change resulted

in data that showed just how these impacts influence the water cycle. With LULC change occurring in the particular regions of the North River watershed, important changes in specific hydrologic components of the water cycle were isolated. Delving into this level of detail with specific water balance components of the water cycle is extremely helpful when developing watershed policies that many regions lack. The results of this study can affirm the scientific consensus within the hydrologic community: increased water yield in deforested scenarios happens through increased surface runoff by alteration of soil water content and percolation rates through removal of deep-rooted vegetation. Reduced water yield occurs in reforested scenarios through increased evapotranspiration leading to alterations in soil water content and percolation as a result of changes in vegetative cover. These patches of different vegetative cover (either deeper rooted young growth trees with greater coverage of canopy vegetation or shrubland/grassland with shallower root networks and less canopy vegetation) influence interception of rainfall and thus surface runoff directly. The increases in surface runoff (>10% over previous LULC scenario) can increase water yield, but can be detrimental to water quality, impair land productivity, reduce the soil's capacity for infiltration and water retention (Aina, 1993). As mentioned, the North River constitutes the majority of the flow into the Lake Tuscaloosa reservoir, highly forested watersheds with intensive forestry can have periodic cycles of cyclic water yield changes. The use of past LULC change over the period of study highlighted realistically occurring LULC change shown versus modelling hypothetical situations, strengthening any use of this study to formulate watershed management policy, especially given sudden clearing, period of recovering forest clearing, with new, rapid regrowth as seen. Spatial and temporal changes in land-cover and the effects on water-balance component interaction is unique to each watershed and assessments of individual catchments are needed to fully grasp the

parameter interaction with not just LULC change, but any climatic changes as well. Results have shown that gross LULC conversions from forest to non-forest and vice versa (with little to no net change as seen with the 2004 to 2006 NLCD change scenario) can lead to large variation in seasonal discharge without typical climatic variation, a subject that will require further testing. This study builds off the trend of increasing intensive forestry in the Southeastern U.S., with a focus on synthesis of forest regrowth in conjunction with forest clearing to assess the water-balance of an important source for recharge of a reservoir.

Limitations

The largest constraint presented in this study is the use of non-annual land-cover data through the NLCD produced by the MRLC, although the NLCD provides 2 to 3-year temporal resolution. Annual land-cover data would assist in further analysis of hydrologic parameter lags between yearly LULC change as well as improve calibration techniques. At a yearly annual resolution, the timing of LULC change would be more precise as well as give more data points in order to run more statistical analysis of specific land-cover patches. As shown by Hernandez et al. (2018), using annual LULC change data versus the original 5-year increment provided by the 1992, 2001, 2006, and 2011 NLCD LULC map (prior to the addition of 2004, 2008, 2013, and 2016) improved prediction of streamflow through the addition of different HRUs to model annual changes. Use of annual forest LULC change maps to track forest removal or regrowth, in theory, allow for more accurate prediction of streamflow. In addition, NLCD products have had some minor misclassification of differing forest types (deciduous versus evergreen) producing some potential differences in the evapotranspiration calculation of SWAT. The limitation of pinpointing specific forest clearings within the watershed and effect on discharge with relation to distance from stream channel or rate of change is greater with non-annual land-cover data.

The reason for opting for the use of the NLCD are as follows: the NLCD has a standardized classification algorithm with average accuracy of >85% with a sufficient temporal time scale of 2 to 3-years to capture major LULC change for the purpose of this study. Because the purpose of this research is to capture the hydrologic response to LULC change, specifically forest to non-forest or the reversal of that trend, the average forest-plantation cycle is caught by the 2-to 3-year NLCD interval. With the increased frequency of LULC updates in the latest NLCD product release, the newest product has higher accuracy than previously released NLCD, as reported by Yang et al (2018), allowing for improved calibration, validation, and prediction over the 5-year NLCD intervals used by Hernandez et al (2018). The CN of differing forest types are quite small, which is used to calculate the rainfall-runoff curve in the water balance calculation in SWAT, meaning that any misclassifications between different forest types will not hamper water-balance and discharge simulations. The succession of forest to grassland/shrub/developed-open developed back to forest, which is typical of intensive forestry in the Southeast U.S., is easily identified by the NLCD without losing the high accuracy of classification. Acquisition of quality, cloud-free Landsat data, classification of annual Landsat data, development of individual SWAT models for the period of study, as well as calibration/validation of the SWAT models would present a time constraint that would not be acceptable for the project. With ample literature on the study of interannual atmospheric teleconnections and the climatic signature within the Southeastern U.S., the need for annual land-cover data for that is beyond the scope of this study. The use of NLCD has allowed for calibration and validation scores above the reported threshold (NSE: >0.5) for this assessment of the North River watershed using SWAT, thus, showing the NLCD products provide a solid

foundation for successful prediction of LULC change in the North River and effects on discharge without the need of annual data.

In some of the LULC change scenarios requiring further analysis of distance to stream channel statistical testing or patch size analysis, SWAT will prove sufficient in analyzing basin wide LULC change and effects on long-term water-balance. Due to the nature of SWAT being a continuous time step model (meaning it produces long-term yields), immediate and individual responses to the hydrology of the basin caused by specific forest loss or forest gain patches may not be able to be assessed in SWAT alone. In addition, water-balance equations are performed at the HRU level and then summed for the basin. As discussed previously, higher temporal scale LULC input will generate different HRUs allowing for better modelling of realistic LULC occurrences and permitting better analysis of the distribution and timing of forest cover patches and effects on the hydrologic cycle. With that being said, the future work suggested for the 2004 to 2006 LULC change scenario can still be performed, with tentative results, using data and SWAT modelling consistent with the rest of this project.

CONCLUSIONS

This first goal of this study was to assess LULC change patterns and quantify LULC change within the North River watershed in Alabama. The second goal was to use hydrologic modelling to see how the hydrology of the watershed was altered through LULC change. SWAT hydrologic modelling proved to be a useful tool in simplifying the complex hydrologic changes that intensive forestry contributed to within the largely rural and forested watershed. With the climatic signal removed, reductions in watershed forest cover increased water yield, while reducing groundwater recharge; increases in forest cover decreased water yield through reduced runoff and increased evapotranspiration. These changes in hydrology have ramifications not only in watersheds of the Southeastern U.S., but around the country and globe as LULC change is the single most significant action in modifying the earth's surface done by humans (Hooke, 2012). Catchment headwaters are sensitive to changes in LULC and are often considered a bellwether of water security. The economy of the North River watershed, as well as other locations through the Southeast U.S., are driven by forestry, an ever-intensive process that has implications on the local residents economically. The incorporation of scientific findings on how LULC change affect hydrology with policies that drive the LULC change will help synthesize a solution that benefits the local population who use the resources of the watershed.

Some of the future work that would further benefit and bolster the findings of this study would be to incorporate the findings of meteorological teleconnections, which have significant influences on the water yield of the watershed. Being able to combine the findings of LULC

change with the meteorological oscillations would give a more complete overview. With this, a more holistic watershed policy would be able to be developed and implemented with the knowledge of how LULC and climate interacts with the goal of maintaining water yield for public use. With proper management of watersheds across the country, water-security issues would be reduced and many of the problems associated with LULC change would be minimized. With the growing concern of water shortages caused by the mismanagement of resources around the world, it is of the utmost importance to further study this topic.

REFERENCES

Abbaspour, K. (2015). *Swat-Cup: Calibration and Uncertainty Programs - A User Manual*. *SWAT-CUP: Calibration and Uncertainty Programs - A User Manual*. Retrieved from https://swat.tamu.edu/media/114860/usermanual_swatcup.pdf

Aina, P. O. (1993). Chapter 1: Rainfall runoff management techniques for erosion control and soil moisture conservation. In *Soil tillage in Africa: needs and challenges*. Retrieved from http://www.fao.org/3/t1696e/T1696e00.htm#TopOfPage

Arceo, M. G. A. S., Cruz, R. V. O., Tiburan Jr., C. L., Balatibat, J. B., & Alibuyog, N. R. (2018). Modeling the Hydrologic Responses to Land Cover and Climate Changes of Selected Watersheds in the Philippines Using Soil and Water Assessment Tool (SWAT) Model. *DLSU Business & Economics Review*, *28*, 84–101.

Arnold, J. G., Srinivasan, R., Muttiah, R. S., & Williams, J. R. (1998). Large Area Hydrologic Modeling And Assessment Part I: Model Development. *Journal of the American Water Resources Association*, 34(1), 73-89. doi:10.1111/j.1752-1688.1998.tb05961.x

Arnold, J. G., Kiniry, J. R., Srinivasan, R., Williams, J. R., Haney, E. B., & Neitsch, S. L. (2012). SWAT Input/Output Documentation. Retrieved from https://swat.tamu.edu/media/69296/swat-io-documentation-2012.pdf.

American FactFinder - U.S. Census. (2010, October 05). Retrieved May 9, 2019, from https://factfinder.census.gov/faces/tableservices/jsf/pages/productview.xhtml?src=bkmk

Anderson, J. R., Hardy, E. E., Roach, J. T., & Witmer, R. E. (1976). A land use and land cover classification system for use with remote sensor data. *Professional Paper*. doi: 10.3133/pp964

Asaro, C., Nowak, J. T., & Elledge, A. (2017). Why have southern pine beetle outbreaks declined in the southeastern U.S. with the expansion of intensive pine silviculture? A brief review of hypotheses. *Forest Ecology and Management*, *391*, 338–348. doi: 10.1016/j.foreco.2017.01.035

Blackmon, M. L., Lee, Y.-H., Wallace, J. M., & Hsu, H.-H. (1984). Time Variation of 500 mb Height Fluctuations with Long, Intermediate and Short Time Scales as Deduced from Lag-Correlation Statistics. *Journal of the Atmospheric Sciences*, *41*(6), 981–991. doi: 10.1175/1520-0469(1984)041<0981:tvomhf>2.0.co;2

Campbell, J. L., Driscoll, C. T., Pourmokhtarian, A., & Hayhoe, K. (2011). Streamflow responses to past and projected future changes in climate at the Hubbard Brook Experimental Forest, New Hampshire, United States. *Water Resources Research*, 47(2). doi:10.1029/2010wr00943

Chitwood, F. (2016). WHO OWNS ALABAMA'S COOSA RIVER? CITIZENS' IMPACT ON THE TRI-STATE WATER WARS MUTED BY PRIVATE OWNERSHIP OF RIPARIAN RIGHTS. *Virginia Environmental Law Journal*, *34*(2), 230–254.

Choto, M., & Fetene, A. (2019). Impacts of land use/land cover change on stream flow and sediment yield of Gojeb watershed, Omo-Gibe basin, Ethiopia. *Remote Sensing Applications: Society and Environment*, *14*, 84–99. doi: 10.1016/j.rsase.2019.01.003

Craig, C., Feng, S., & Gilbertz, S. (2019). Water crisis, drought, and climate change in the southeast United States. *Land Use Policy*, *88*, 104110. doi: 10.1016/j.landusepol.2019.104110

Dahlman, L. (2009, August 30). Climate Variability: Arctic Oscillation. Retrieved from https://www.climate.gov/news-features/understanding-climate/climate-variability-arctic-oscillation

Drion, E. F. (1952). Some Distribution-Free Tests for the Difference Between two Empirical Cumulative Distribution Functions. *The Annals of Mathematical Statistics*, *23*(4), 563–574. doi: 10.1214/aoms/1177729335

Drummond, M. A., Stier, M. P., Auch, R. F., Taylor, J. L., Griffith, G. E., Riegle, J. L., … Mcbeth, J. L. (2015). Assessing Landscape Change and Processes of Recurrence, Replacement, and Recovery in the Southeastern Coastal Plains, USA. *Environmental Management*, *56*(5), 1252–1271. doi: 10.1007/s00267-015-0574-1

Economic Impacts of Alabama's Agricultural, Forestry, and Related Industries. *Economic Impacts of Alabama's Agricultural, Forestry, and Related Industries*. (2013). Auburn University. Retrieved from http://www.forestry.alabama.gov/Pages/Management/Forms/Economic_Impact.pdf

Enfield, D. B., Mestas-Nuñez, A. M., & Trimble, P. J. (2001). The Atlantic Multidecadal Oscillation and its relation to rainfall and river flows in the continental U.S. *Geophysical Research Letters*, *28*(10), 2077–2080. doi: 10.1029/2000gl012745

Engström, J., & Waylen, P. (2017). The changing hydroclimatology of Southeastern U.S. *Journal of Hydrology*, 548, 16-23. doi:10.1016/j.jhydrol.2017.02.039

Engström, J., & Waylen, P. (2018). Drivers of long-term precipitation and runoff variability in the southeastern USA. *Theoretical and Applied Climatology*, 131(3-4), 1133-1146. doi:10.1007/s00704-016-2030-4

Fry, J. A., Coan, M. J., Homer, C. G., Meyer, D. K., & Wickham, J. D. (2008). Completion of the National Land Cover Database (NLCD) 1992–2001 Land Cover Change Retrofit Product (Tech. No. 1379). Retrieved May 26, 2019, from https://pubs.usgs.gov/of/2008/1379/pdf/ofr2008-1379.pdf.

Garen, D. C., & Moore, D. S. (2005). REPLY TO DISCUSSION by M. Todd Walter and Stephen B. Shaw. *Journal of the American Water Resources Association*, 41(6), 1493-1494. doi:10.1111/j.1752-1688.2005.tb03816.x

Gassman, P. W., Reyes, M. R., Green, C. H., & Arnold, J. G. (2007). The Soil and Water Assessment Tool: Historical Development, Applications, and Future Research Directions. *Transactions of the ASABE*, 50(4), 1211-1250. doi:10.13031/2013.23637

Githui, F., Mutua, F., & Bauwens, W. (2009). Estimating the impacts of land-cover change on runoff using the soil and water assessment tool (SWAT): case study of Nzoia catchment, Kenya / Estimation des impacts du changement doccupation du sol sur lécoulement à laide de SWAT: étude du cas du bassin de Nzoia, Kenya. *Hydrological Sciences Journal*, *54*(5), 899–908. doi: 10.1623/hysj.54.5.899

Gleick, P. H., 1996: Water resources. In Encyclopedia of Climate and Weather, ed. by S. H. Schneider, Oxford University Press, New York, vol. 2, pp. 817-823.

Global Weather Data for SWAT. Retrieved from https://globalweather.tamu.edu/

Gong, H., Pan, Y., & Xu, Y. (2012). Spatio-temporal variation of groundwater recharge in response to variability in precipitation, land use and soil in Yanqing Basin, Beijing, China. *Hydrogeology Journal*, *20*(7), 1331–1340. doi: 10.1007/s10040-012-0883-x

Grace, J., Jose´, J.S., Meir, P., Miranda, H.S. & Montes, R.A. (2006) Productivity and carbon fluxes of tropical savannas. *Journal of Biogeography*, 33, 387–400

Graham, M. E., & Congalton, R. G. (2009). A Comparison of the 1992 and 2001 National Land Cover Datasets in the Lamprey River Watershed, NH [Conference Presentation]. Retrieved May 26, 2019, from https://www.asprs.org/wp-content/uploads/2010/12/Graham.pdf

Griffiths, N. A., Jackson, C. R., Bitew, M. M., Fortner, A. M., Fouts, K. L., Mccracken, K., & Phillips, J. R. (2017). Water quality effects of short-rotation pine management for bioenergy feedstocks in the southeastern United States. *Forest Ecology and Management*, 400, 181-198. doi:10.1016/j.foreco.2017.06.011

Hernandez, A., Healey, S., Huang, H., & Ramsey, R. (2018). Improved Prediction of Stream Flow Based on Updating Land Cover Maps with Remotely Sensed Forest Change Detection. *Forests*, *9*(6), 317. doi: 10.3390/f9060317

Homer, C., Dewitz, J., Fry, J., Coan, M., Hossain, N., Larson, C., Herold, N., McKerrow, J., VanDriel, N., & Wickham, J. (2007). Completion of the 2001 National Land Cover Database for the Counterminous United States. *Photogrammetric Engineering and Remote Sensing*, 73(4), 337.

Hong, Y., & Adler, R. F. (2008). Estimation of global SCS curve numbers using satellite remote sensing and geospatial data. *International Journal of Remote Sensing*, 29(2), 471-477. doi:10.1080/01431160701264292

Hooke, R. L., & Martín-Duque, J. F. (2012). Land transformation by humans: A review. *GSA Today, 12*(12), 4–10. doi: 10.1130/gsat151a.1

Hurrell, J. W. (2003). *The North Atlantic oscillation: climatic significance and environmental impact*. Washington, DC: American Geophysical Union.

Ide, J. I., Finér, L., Laurén, A., Piirainen, S., & Launiainen, S. (2013). Effects of clear-cutting on annual and seasonal runoff from a boreal forest catchment in eastern Finland. *Forest Ecology and Management, 304*, 482–491. doi: 10.1016/j.foreco.2013.05.051

Kalcic, M. M., Chaubey, I., & Frankenberger, J. (2015). Defining Soil and Water Assessment Tool (SWAT) hydrologic response units (HRUs) by field boundaries. International *Journal of Agricultural and Biological Engineers*, 8(3). Retrieved from http://www.ijabe.org/index.php/ijabe/article/view/951

Katz, R. W., Parlange, M. B., & Tebaldi, C. (2003). Stochastic Modeling of the Effects of Large-Scale Circulation on Daily Weather in the Southeastern U.S. Issues in the Impacts of Climate Variability and Change on Agriculture, 189-216. doi:10.1007/978-94-017-1984-1_9

Kim, N. W., Lee, J. W., Lee, J., & Lee, J. E. (2010). SWAT application to estimate design runoff curve number for South Korean conditions. *Hydrological Processes*. doi:10.1002/hyp.7638

Kolmogorov-Smirnov test. - MIT OpenCourseWare. Retrieved from https://ocw.mit.edu/courses/mathematics/18-443-statistics-for-applications-fall-2006/lecture-notes/lecture14.pdf

Laiho, R., Sanchez, F., Tiarks, A., Dougherty, P. M., & Trettin, C. C. (2003). Impacts of intensive forestry on early rotation trends in site carbon pools in the southeastern US. *Forest Ecology and Management*, 174(1-3), 177-189. doi:10.1016/s0378-1127(02)00020-8

Leathers, D. J., Yarnal, B., & Palecki, M. A. (1991). The Pacific/North American Teleconnection Pattern and United States Climate. Part I: Regional Temperature and Precipitation Associations. *Journal of Climate*, *4*(5), 517–528. doi: 10.1175/1520-0442(1991)004<0517:tpatpa>2.0.co;2

Li, D., & Xiao, Z. (2018). Can solar cycle modulate the ENSO effect on the Pacific/North American pattern? *Journal of Atmospheric and Solar-Terrestrial Physics*, 167, 30-38. doi:10.1016/j.jastp.2017.10.007

Mango, L. M., Melesse, A. M., Mcclain, M. E., Gann, D., & Setegn, S. G. (2011). Land use and climate change impacts on the hydrology of the upper Mara River Basin, Kenya: results of a modeling study to support better resource management. *Hydrology and Earth System Sciences*, *15*(7), 2245–2258. doi: 10.5194/hess-15-2245-2011

Massa, S. Retrieved from http://www.stats.ox.ac.uk/~massa/Lecture 13.pdf

Massey, F. J. (1951). The Kolmogorov-Smirnov Test for Goodness of Fit. *Journal of the American Statistical Association*, *46*(253), 68. doi: 10.2307/2280095

Mccuen, R. H., Knight, Z., & Cutter, A. G. (2006). Evaluation of the Nash–Sutcliffe Efficiency Index. *Journal of Hydrologic Engineering*, 11(6), 597-602. doi:10.1061/(asce)1084-0699(2006)11:6(597)

Moriasi, D. N., Arnold, J. G., Liew, M. W., Bingner, R. L., Harmel, R. D., & Veith, T. L. (2007). Model Evaluation Guidelines for Systematic Quantification of Accuracy in Watershed Simulations. *Transactions of the ASABE*, 50(3), 885-900. doi:10.13031/2013.23153

Nash, J., & Sutcliffe, J. (1970). River flow forecasting through conceptual models part I — A discussion of principles. *Journal of Hydrology*, *10*(3), 282–290. doi: 10.1016/0022-1694(70)90255-6

Neitsch, S. L., Arnold, J. G., Kiniry, J. R., & Williams, J. R. (2011). Soil and Water Assessment Tool Theoretical Documentation Version 2009 (Tech. No. TR-406 2011). Retrieved June 20, 2019, from Texas A&M College of Agriculture and Life Sciences website: https://swat.tamu.edu/media/99192/swat2009-theory.pdf

Norrell, R. J., & Gomillion, C. G. (2019). Alabama. In Encyclopedia Britannica. Retrieved May 31, 2019, from https://www.britannica.com/place/Alabama-state

NRCS: Geospatial Data Gateway: Home. Retrieved from https://datagateway.nrcs.usda.gov/

O'Neill, P. E., McGregor, S. W., & Wynn, E. A. (2010). WATERSHED ASSESSMENT OF THE NORTH RIVER SYSTEM FOR RECOVERY AND RESTORATION OF RARE MUSSEL SPECIES (Rep. No. 0918). Retrieved May 31, 2019, from GEOLOGICAL SURVEY OF ALABAMA website: https://gsa.state.al.us/img/Ecosystems/pdf/OFR_0918.pdf

Park, K. I. (2018). *Fundamentals of Probability and Stochastic Processes with Applications to Communications*. Cham: Springer International Publishing.

Portmann, R. W., Solomon, S., & Hegerl, G. C. (2009). Spatial and seasonal patterns in climate change, temperatures, and precipitation across the United States. *Proceedings of the National Academy of Sciences,* 106(18), 7324-7329. doi:10.1073/pnas.0808533106

Price, K. (2011). Effects of watershed topography, soils, land use, and climate on baseflow hydrology in humid regions: A review. *Progress in Physical Geography: Earth and Environment*, 35(4), 465-492. doi:10.1177/0309133311402714

Quyen, N. T., Liem, N. D., & Loi, N. K. (2014). Effect of land use change on water discharge in Srepok watershed, Central Highland, Viet Nam. *International Soil and Water Conservation Research*, 2(3), 74-86. doi:10.1016/s2095-6339(15)30025-3

Rasmusson, E. M., & Wallace, J. M. (1983). Meteorological Aspects of the El Nino/Southern Oscillation. *Science*, *222*(4629), 1195–1202. doi: 10.1126/science.222.4629.1195

Roundy, J. K., Yuan, X., Schaake, J., & Wood, E. F. (2015). A Framework for Diagnosing Seasonal Prediction through Canonical Event Analysis. *Monthly Weather Review*, *143*(6), 2404–2418. doi: 10.1175/mwr-d-14-00190.1

Reinhardt-Imjela, C., Imjela, R., Bölscher, J., & Schulte, A. (2018). The impact of late medieval deforestation and 20th century forest decline on extreme flood magnitudes in the Ore Mountains (Southeastern Germany). *Quaternary International*, *475*, 42–53. doi: 10.1016/j.quaint.2017.12.010

Ruxton, G. D. (2006). The unequal variance t-test is an underused alternative to Students t-test and the Mann–Whitney U test. *Behavioral Ecology*, *17*(4), 688–690. doi: 10.1093/beheco/ark016

Schlesinger, M. E., & Ramankutty, N. (1994). An oscillation in the global climate system of period 65–70 years. *Nature*, *367*(6465), 723–726. doi: 10.1038/367723a0

Shrestha, B. B. (2019). Approach for Analysis of Land-Cover Changes and Their Impact on Flooding Regime. *Quaternary*, *2*(3), 27. doi: 10.3390/quat2030027

Singh, D., Mcdermid, S. P., Cook, B. I., Puma, M. J., Nazarenko, L., & Kelley, M. (2018). Distinct Influences of Land Cover and Land Management on Seasonal Climate. *Journal of Geophysical Research: Atmospheres*, 123(21). doi:10.1029/2018jd028874

Sitterson, J., Knightes, C., Parmar, R., Wolfe, K., Muche, M., & Avant, B. (2017). An Overview of Rainfall-Runoff Model Types (Rep.). Retrieved from file:///C:/Users/oit/Downloads/FINAL_RUNOFF_MODELS_SITTERSON 508 REVISED.PDF

Slack, L. J. (1987). WATER QUALITY OF LAKE TUSCALOOSA AND STREAMFLOW AND WATER QUALITY OF SELECTED TRIBUTARIES TO LAKE TUSCALOOSA,

ALABAMA (Tech. No. 87-4002). Retrieved May 31, 2019, from https://pubs.usgs.gov/wri/1987/4002/report.pdf

Sokal, R. R., & Rohlf, F. J. (1987). *Introduction to biostatistics*. New York: W.H. Freeman.

"Station Name: AL TUSCALOOSA MUNI AP". National Oceanic and Atmospheric Administration. Retrieved 2013-03-09.

Sun, G., Caldwell, P. V., & Mcnulty, S. G. (2015). Modelling the potential role of forest thinning in maintaining water supplies under a changing climate across the conterminous United States. *Hydrological Processes*, *29*(24), 5016–5030. doi: 10.1002/hyp.10469

Suttles, K. M., Singh, N. K., Vose, J. M., Martin, K. L., Emanuel, R. E., Coulston, J. W., . . . Crump, M. T. (2018). Assessment of hydrologic vulnerability to urbanization and climate change in a rapidly changing watershed in the Southeast U.S. *Science of The Total Environment*, 645, 806-816. doi:10.1016/j.scitotenv.2018.06.287

Szcześniak, M., & Piniewski, M. (2015). Improvement of Hydrological Simulations by Applying Daily Precipitation Interpolation Schemes in Meso-Scale Catchments. *Water*, 7(12), 747-779. doi:10.3390/w7020747

Tamm, O., Maasikamäe, S., Padari, A., & Tamm, T. (2018). Modelling the effects of land use and climate change on the water resources in the eastern Baltic Sea region using the SWAT model. *Catena*, 167, 78-89. doi:10.1016/j.catena.2018.04.029

Tan, Gassman, Srinivasan, Arnold, & Yang. (2019). A Review of SWAT Studies in Southeast Asia: Applications, Challenges and Future Directions. *Water*, 11(5), 914. doi:10.3390/w11050914

Tasdighi, A., Arabi, M., & Harmel, D. (2018). A probabilistic appraisal of rainfall-runoff modeling approaches within SWAT in mixed land use watersheds. *Journal of Hydrology*, 564, 476-489. doi:10.1016/j.jhydrol.2018.07.035

Teklay, A., Dile, Y. T., Setegn, S. G., Demissie, S. S., & Asfaw, D. H. (2019). Evaluation of static and dynamic land use data for watershed hydrologic process simulation: A case study in Gummara watershed, Ethiopia. *Catena*, 172, 65-75. doi:10.1016/j.catena.2018.08.013

Thavhana, M., Savage, M., & Moeletsi, M. (2018). SWAT model uncertainty analysis, calibration and validation for runoff simulation in the Luvuvhu River catchment, South Africa. *Physics and Chemistry of the Earth, Parts A/B/C*, 105, 115-124. doi:10.1016/j.pce.2018.03.012

Thompson, D. W. J., & Wallace, J. M. (1998). The Arctic oscillation signature in the wintertime geopotential height and temperature fields. *Geophysical Research Letters*, *25*(9), 1297–1300. doi: 10.1029/98gl00950

Tyagi, J. V., & Rao, Y. R. S. (n.d.). Retrieved from https://swat.tamu.edu/media/115946/3-jaivir-tyagi-e3-session.pdf

United States, Department of Natural Resources. Silviculture Handbook. Retrieved May 30, 2019, from https://dnr.wi.gov/topic/ForestManagement/documents/24315/21.pdf

USGS National Land Cover Dataset (NLCD) Downloadable Data Collection. (2018, August 01). Retrieved from https://catalog.data.gov/dataset/usgs-national-land-cover-dataset-nlcd-downloadable-data-collection

USGS Stream gage Data. Retrieved from https://waterdata.usgs.gov/al/nwis/uv/?site_no=02464000&PARAmeter_cd=00065,00060

Vertessy, R. A., Watson, F. G., & O′sullivan, S. K. (2001). Factors determining relations between stand age and catchment water balance in mountain ash forests. *Forest Ecology and Management*, 143(1-3), 13-26. doi:10.1016/s0378-1127(00)00501-6

Wahren, A., Schwärzel, K., & Feger, K.-H. (2012). Potentials and limitations of natural flood retention by forested land in headwater catchments: evidence from experimental and model studies. *Journal of Flood Risk Management*, *5*(4), 321–335. doi: 10.1111/j.1753-318x.2012.01152.x

Wang, H., Tetzlaff, D., & Soulsby, C. (2018). Modelling the effects of land cover and climate change on soil water partitioning in a boreal headwater catchment. *Journal of Hydrology*, *558*, 520–531. doi: 10.1016/j.jhydrol.2018.02.002

Wang, Q., Liu, R., Men, C., Guo, L., & Miao, Y. (2018). Effects of dynamic land use inputs on improvement of SWAT model performance and uncertainty analysis of outputs. *Journal of Hydrology*, 563, 874-886. doi:10.1016/j.jhydrol.2018.06.063

Ward, E. J., Oren, R., Kim, H. S., Kim, D., Tor-Ngern, P., Ewers, B. E., … Schäfer, K. V. R. (2018). Evapotranspiration and water yield of a pine-broadleaf forest are not altered by long-term atmospheric [CO2] enrichment under native or enhanced soil fertility. *Global Change Biology*, *24*(10), 4841–4856. doi: 10.1111/gcb.14363

Watson, J. E. M., Dudley, N., Segan, D. B., & Hockings, M. (2014). The performance and potential of protected areas. *Nature*, *515*(7525), 67–73. doi: 10.1038/nature13947

Wheater, H. S., & Gober, P. (2015). Water security and the science agenda. *Water Resources Research*, *51*(7), 5406–5424. doi: 10.1002/2015wr016892

Whittaker, G., Confesor, R., Jr., Luzio, M. D., & Arnold, J. G. (2010). Detection of Overparameterization and Overfitting in an Automatic Calibration of SWAT. *Transactions of the ASABE*, 53(5), 1487-1499. doi:10.13031/2013.34909

Wickham, J., Stehman, S., Smith, J., & Yang, L. (2004). Thematic accuracy of the 1992 National Land-Cover Data for the western United States. *Remote Sensing of Environment*, 91(3-4), 452-468. doi:10.1016/j.rse.2004.04.002

Wickham, J. D., Stehman, S. V., Gass, L., Dewitz, J., Fry, J. A., & Wade, T. G. (2013). Accuracy assessment of NLCD 2006 land cover and impervious surface. *Remote Sensing of Environment*, 130, 294-304. doi:10.1016/j.rse.2012.12.001

Wickham, J., Stehman, S., Gass, L., Dewitz, J., Sorenson, D., Granneman, B., Poss, R., & Baer, L. (2017). Thematic accuracy assessment of the 2011 National Land-Cover Database (NLCD). *Remote Sensing of Environment*, 191, 328-341. doi: 10.1016/j.rse.2016.12.026

Xian, G., & Homer, C. (2010). Updating the 2001 National Land Cover Database Impervious Surface Products to 2006 using Landsat Imagery Change Detection Methods. *Remote Sensing of Environment*, 114(8), 1676-1686. doi:10.1016/j.rse.2010.02.018

Yaduvanshi, A., Srivastava, P., Worqlul, A., & Sinha, A. (2018). Uncertainty in a Lumped and a Semi-Distributed Model for Discharge Prediction in Ghatshila Catchment. *Water*, 10(4), 381. doi:10.3390/w10040381

Yamazaki, K., Ogi, M., Tachibana, Y., Nakamura, T., & Oshima, K. (2019). Recent Breakdown of the Seasonal Linkage between the Winter North Atlantic Oscillation/Northern Annular Mode and Summer Northern Annular Mode. *Journal of Climate*, *32*(2), 591–605. doi: 10.1175/jcli-d-17-0820.1

Yang, L., Jin, S., Danielson, P., Homer, C., Gass, L., Bender, S. M., … Xian, G. (2018). A new generation of the United States National Land Cover Database: Requirements, research priorities, design, and implementation strategies. *ISPRS Journal of Photogrammetry and Remote Sensing*, 146, 108–123. doi: 10.1016/j.isprsjprs.2018.09.00

Zhang, D., Zhang, Q., Qiu, J., Bai, P., Liang, K., & Li, X. (2018). Intensification of hydrological drought due to human activity in the middle reaches of the Yangtze River, China. *Science of The Total Environment*, *637-638*, 1432–1442. doi: 10.1016/j.scitotenv.2018.05.121

Zipper, S. C., Motew, M., Booth, E. G., Chen, X., Qiu, J., Kucharik, C. J., … Ii, S. P. L. (2018). Continuous separation of land use and climate effects on the past and future water balance. *Journal of Hydrology*, *565*, 106–122. doi: 10.1016/j.jhydrol.2018.08.022